

IDENTIFICATION AND RESTORATION OF A CLASS OF ALIASED SIGNALS

by

Aasma Walia

BTech, G. G. S. Indraprastha University, 2002

Submitted to the Graduate Faculty of
the School of Engineering in partial fulfillment
of the requirements for the degree of

Master of Science

University of Pittsburgh

2004

UNIVERSITY OF PITTSBURGH
SCHOOL OF ENGINEERING

This thesis was presented

by

Aasma Walia

It was defended on

April 6, 2004

and approved by

Patrick Loughlin, Professor, Electrical Engineering Department

Amro A. El-Jaroudi, Associate Professor, Electrical Engineering Department

L. F. Chaparro, Associate Professor, Electrical Engineering Department

Thesis Advisor: Patrick Loughlin, Professor, Electrical Engineering Department

IDENTIFICATION AND RESTORATION OF A CLASS OF ALIASED SIGNALS

Aasma Walia, M.S.

University of Pittsburgh, 2004

A fundamental theorem of Digital Signal Processing is Shannon's sampling theorem, which dictates the minimum rate (called the "Nyquist rate") at which a continuous-time signal must be sampled in order to faithfully reproduce the signal from its samples. If a signal can be reproduced from its samples, then clearly no information about the original signal has been lost in the sampling process. However, when a signal is sampled at a rate lower than the Nyquist Rate, the true spectral content of the original signal is distorted due to "aliasing," wherein frequencies in the original signal greater than the sampling frequency appear as lower frequencies in the sampled signal. This distortion is generally held to be irrecoverable, i.e., whenever aliasing occurs, information is considered to be inevitably lost.

This research challenges this notion and presents a technique for identifying aliasing and recovering an unaliased version of a signal from its aliased samples. The method is applicable to frequency-modulated (FM) signals with a continuous instantaneous frequency (IF), and utilizes analysis of the IF of the aliased signal to 1) determine whether the signal has potentially been aliased and, if so, 2) compensate for the aliasing by reconstructing an estimate of the true IF of the signal. Time-frequency methods are used to analyze the potentially aliased signal and estimate the IF, together with modulation, re-sampling and interpolation stages to reconstruct an estimate of the unaliased signal. The proposed technique can yield excellent reconstruction of FM signals given ideal estimates of the IF.

TABLE OF CONTENTS

1.0 INTRODUCTION	1
1.1 Sampling and Aliasing	2
2.0 TIME-FREQUENCY DISTRIBUTIONS	4
2.1 Introduction	4
2.2 Continuous TFDs	4
2.2.1 Wigner Distribution	4
2.2.2 Cohen's General Class of TFDs	5
2.2.3 Spectrogram	6
2.3 Discrete-time Time Frequency Distribution (DTFD)	7
2.4 Discrete-time Wigner Distribution (DWD)	7
2.4.1 Relationship between Discrete and Continuous WD	7
2.5 Instantaneous Frequency	8
3.0 INTRODUCTION OF THE METHOD TO IDENTIFY POTENTIAL ALIASING, AND COMPENSATE FOR IT	11
3.1 Illustration of the Method	15
3.1.1 Step 1: Analytic Signal	17
3.1.2 Step 2: Spectrogram	17
3.1.3 Step 3: Instantaneous Frequency	18
3.1.4 Step 4: Instantaneous Frequency Correction	19
3.1.5 Step 5: Phase Estimation	21
3.1.6 Step 6: Demodulation	22
3.1.7 Step 7: Upsampling	23
3.1.8 Step 8: Reconstruction	24
4.0 RESULTS AND DISCUSSION	25
4.1 Ideal Cases	28
4.2 Non-Ideal Cases	35
4.3 A Few Limitations	35
4.4 Analysis of "Turns" in IF	42
4.5 Application : Multi-component Signals	47
4.6 IF Estimate and other sources of Error	51
APPENDIX. SOURCE CODE	54
BIBLIOGRAPHY	57

LIST OF FIGURES

3.1	Unaliased WD of Chirp Signal. Gray region represents the observed range of the DTWD	12
3.2	Aliased WD of Chirp Signal (Exponential). Now over the time interval that we observed the signal (gray region), we see a sudden discontinuity in the trajectory when the IF greater than $F_s/2$	13
3.3	Aliased WD of Chirp Signal (Real)	13
3.4	Aliased WD of Chirp Signal (Analytic)	14
3.5	(a) Time-series and (b) Log-magnitude spectrogram of the aliased signal . . .	15
3.6	Block diagram of a method to compensate for aliasing	16
3.7	Log-Magnitude Spectrogram of the Analytic Signal $y[n]$	17
3.8	Original IF Estimates for the Analytic Signal $y[n]$	19
3.9	Corrected IF Estimates for the Analytic Signal $y(t)$	20
3.10	Phase Estimates for the (a) original and (b) corrected IF estimates	21
3.11	Demodulated Signal	22
3.12	(a) Phase signal with upsampled corrected phase and (b) upsampled demodulated signal	23
3.13	Reconstructed signal	24
4.1	Ideal Case 1: Constant Amplitude, Log-magnitude spectrogram of (a) the aliased signal, (b) the analytic signal, (c) upsampled demodulated signal, (d) phase signal with corrected phase and (e) reconstructed signal	29
4.2	Ideal Case 1: Constant Amplitude, (a) Log-magnitude spectrogram of the restored signal (b) log-magnitude spectrogram of the “true” unaliased signal (with correct sampling rate) (c) error between (a) and (b). Time-series of the (d) reconstructed signal, (e) “true” unaliased signal (with correct sampling rate) and (f) the error between (d) and (e)	30

4.3	Ideal Case 2: Gaussian Amplitude, Log-magnitude spectrogram of (a) the aliased signal, (b)the analytic signal, (c) upsampled demodulated signal, (d) phase signal with corrected phase and (e) reconstructed signal	31
4.4	Ideal Case 2: Gaussian Amplitude, (a) Log-magnitude spectrogram of the restored signal (b) log-magnitude spectrogram of the “true” unaliased signal (with correct sampling rate) (c) error between (a) and (b). Time-series of the (d) reconstructed signal, (e) “true” unaliased signal (with correct sampling rate) and (f) the error between (d) and (e)	32
4.5	Ideal Case 3: Sinusoidal Amplitude, Log-magnitude spectrogram of (a) the aliased signal, (b)the analytic signal, (c) upsampled demodulated signal, (d) phase signal with corrected phase and (e) reconstructed signal	33
4.6	Ideal Case 3: Sinusoidal Amplitude, (a) Log-magnitude spectrogram of the restored signal (b) log-magnitude spectrogram of the “true” unaliased signal (with correct sampling rate) (c) error between (a) and (b). Time-series of the (d) reconstructed signal, (e) “true” unaliased signal (with correct sampling rate) and (f) the error between (d) and (e)	34
4.7	Case 1: Gaussian Amplitude, Log-magnitude spectrogram of (a) the aliased signal, (b)the analytic signal, (c) demodulated signal, (d) phase signal with corrected phase, (e) reconstructed signal and (f) unaliased signal (with correct sampling rate)	36
4.8	Case 2: Sinusoidal Amplitude, Log-magnitude spectrogram of (a) the aliased signal, (b)the analytic signal, (c) demodulated signal, (d) phase signal with corrected phase, (e) reconstructed signal and (f) unaliased signal (with correct sampling rate)	37
4.9	Case 3: Amplitude as a Combination of Sinusoids : Log-magnitude spectrogram of (a) the Aliased signal, (b)the analytic signal, (c) demodulated signal, (d) phase signal with corrected phase, (e) reconstructed signal and (f) unaliased signal (with correct sampling rate)	38
4.10	Case 4: Cubic Phase, Log-magnitude spectrogram of (a) the Aliased signal, (b)the analytic signal, (c) demodulated signal, (d) phase signal with corrected phase, (e) reconstructed signal and (f) unaliased signal (with correct sampling rate)	39
4.11	Case 6: Aliasing with Multiple Turns, Log-magnitude spectrogram of (a) the aliased signal, (b)the analytic signal, (c) demodulated signal, (d) phase signal with corrected phase, (e) reconstructed signal and (f) unaliased signal (with correct sampling rate)	40
4.12	Log-magnitude spectrogram of (a) Signal with discontinuous trajectory and (b) its analytic signal	41

4.13 Aliased analytic signal	42
4.14 (a) Ideal IF for the aliased signal and (b) its derivative	43
4.15 (a) Unaliased analytic signal, (b) its ideal IF and (c) first derivative of IF	44
4.16 (a) First derivative of the original IF estimates and (b) its “smoothed” version	45
4.17 (a) First derivative of the corrected IF estimates and (b) its “smoothed” version	45
4.18 (a) Sinusoidal amplitude aliased analytic signal, (b) its IF estimates and (c) smoothed first derivative of the IF estimate	46
4.19 Combination of two chirps: Log-magnitude spectrogram of (a) aliased analytic signal and (b) the analytic signal	47
4.20 Combination of two chirps: Log-magnitude spectrogram of (a) the upsampled low-pass filtered demodulated signal using first phase, and (b) the first reconstructed chirp component	48
4.21 Combination of two chirps: Log-magnitude spectrogram of (a) the upsampled low-pass filtered demodulated signal using second phase, and (b) the second reconstructed chirp component	48
4.22 Combination of two chirps: Log-magnitude spectrogram of the reconstructed signal	49
4.23 Combination of two chirps: (a) Log-magnitude spectrogram of the restored signal (b) log-magnitude spectrogram of the “true” unaliased signal (with correct sampling rate) (c) error between (a) and (b). Time-series of the (d) reconstructed signal, (e) “true” unaliased signal (with correct sampling rate) and (f) the error between (d) and (e)	50
4.24 Quadrature Signal : Log-magnitude spectrogram of (a) the aliased signal, (b) upsampled demodulated signal, (c) phase signal with corrected phase and (d) reconstructed signal	52
4.25 Quadrature Signal : (a) Log-magnitude spectrogram of the restored signal (b) log-magnitude spectrogram of the “true” unaliased signal (with correct sampling rate) (c) error between (a) and (b). Time-series of the (d) reconstructed signal, (e) “true” unaliased signal (with correct sampling rate) and (f) the error between (d) and (e)	53

1.0 INTRODUCTION

Shannon's sampling theorem states that when converting from an analog signal to digital (or otherwise sampling a signal at discrete intervals), the sampling frequency must be greater than twice the highest frequency of the input signal (Nyquist rate) in order to be able to faithfully reconstruct the original signal from the sampled version ¹. If the sampling frequency is less than this limit, then frequencies in the original signal that are above half the sampling rate will be "aliased" and will appear in the resulting signal as lower frequencies. When this happens, the original signal cannot be reconstructed from the sampled signal.

Here, we present a method which attempts to recover a signal after it has been sampled at a rate lower than the Nyquist rate. The method involves obtaining the instantaneous frequency (IF) estimate for the original, potentially aliased, signal. Under conditions when the signal is aliased, the method compensates for this aliasing by correcting the IF estimate and reconstructing an unaliased version of the signal.

This technique attempts to identify and correct for aliasing in a class of signals, having moderate amplitude-modulation and continuous frequency-modulation. For such signals, the time-frequency distribution is concentrated along the instantaneous frequency of the signal, and it is possible to obtain very good estimates for the phase. As derived later, the Wigner distribution for this class of signals can be approximated as:

$$W_s(t, \omega) \approx \frac{A^2(t)}{\sqrt{2\pi\sigma_\omega^2(t)}} e^{(-\frac{(\omega - \phi'(t))^2}{2\sigma_\omega^2(t)})} \quad (1.1)$$

This thesis uses time-frequency techniques to obtain IF estimates. Then the signal is demodulated, upsampled, interpolated, and remodulated by the compensated IF. Under ideal conditions - with perfect IF estimates - the technique reconstructs the unaliased signal given only the aliased version.

¹Bandlimited signals centered about some frequency $\omega_0 > 0$, can be sampled at a rate lower than the Nyquist rate and it is possible to recover the signal if the bandwidth is known.

1.1 SAMPLING AND ALIASING

With the advent of digital computers and their subsequent widespread availability, most analysis of data are now done digitally. Hence the need to convert continuous-time signals, such as speech, music, biomedical signals (EEG, EMG, EKG, etc.), sonar, radar, machine vibrations, etc. into discrete samples that can be manipulated on a digital computer. The rate at which the signals are sampled for subsequent digital analysis is called the *Sampling Rate* or *Sampling Frequency*.

According to the Sampling Theorem, if the signal is band-limited and if the sampling rate is high enough, then the samples uniquely specify the original signal and perfect reconstruction of the original signal from its samples can be achieved. The Sampling Theorem can be stated as:

Let $s(t)$ be a band-limited signal with $S(\omega) = 0$ for $|\omega| > \omega_m$. Then, $s(t)$ is uniquely determined by its samples $s(nT)$, $n = 0, \pm 1, \pm 2, \dots$, if $\omega_s \geq 2\omega_m$.

Here, ω_m is the largest frequency component in $s(t)$, $2\omega_m$ is the Nyquist rate, and ω_s is the sampling frequency. If a band-limited signal has been sampled at a rate greater than or equal to the Nyquist rate, then the continuous signal can be recovered perfectly via interpolation.

But if any band-limited signal has been sampled at a rate lower than the Nyquist rate, then replica overlap in frequency occurs. This undersampling in time, is called *Aliasing*, wherein frequencies above half the sampling frequency appear as lower frequencies in the sampled version of the original signal. Aliasing results in a distorted version of the original signal. The spectrum of the sampled signal after aliasing does not have one-to-one correspondence to that of the original continuous-time signal. Therefore, the spectrum of the sampled signal cannot be used to analyze the continuous time signal and the continuous time signal cannot be uniquely reconstructed from its samples.

Consider a signal $s(t)$, which is sampled using a periodic 1/0 pulse train $p(t)$ with period T and duty cycle of duration τ . Let $s_s(t)$ denote the sampled signal, given by $s_s(t) = p(t)s(t)$. We can represent Fourier transform pairs by

$$s(t) \Leftrightarrow S(\omega) = \int s(t)e^{-j\omega t} dt$$

$$s_s(t) \Leftrightarrow S_s(\omega) = \int s(t)e^{-j\omega t} dt$$

Since $p(t)$ is a periodic function, it can be expressed in terms of a Fourier series,

$$p(t) = \sum_n c_n \exp(jn\omega_s t) \quad (1.2)$$

where

$$c_0 = \frac{1}{T} \int_0^T p(t) dt \quad (1.3)$$

and,

$$c_n = \frac{1}{T} \int_0^T p(t) \exp(-jn\omega_s t) dt \quad n = \pm 1, \pm 2, \dots \quad (1.4)$$

with $\omega_s = 2\pi/T$.

Taking a Fourier transform of $s_s(t)$ and applying the multiplication/convolution property together with the identity

$$\int \exp(j\omega t) dt = 2\pi\delta(\omega) \quad (1.5)$$

we have that

$$S_s(\omega) = c_0 S(\omega) + \sum_{n \neq 0} c_n S(\omega - n\omega_s) \quad (1.6)$$

It can be seen that $S_s(\omega)$ consists of an amplitude-scaled replica of the true spectrum $S(\omega)$ of the original signal, plus a sum of scaled replicas of $S(\omega)$ shifted in frequency by integer multiples of ω_s . Hence, if the shifted replicas do not overlap, which will be the case when ω_s is greater than twice the maximum frequency ω_m in the signal, then aliasing is avoided and the replicas can be removed by filtering. However, when ω_s is less than $2\omega_m$, then the replicas overlap and the original spectrum is distorted and can not be recovered by filtering.

In this thesis we present a new approach that in some cases allows aliasing to be identified and corrected, so that an unaliased version of the original signal can be recovered from the aliased signal. The approach utilizes time-frequency methods to jointly analyze the signal in time and frequency and estimate the instantaneous frequency of the signal. Under certain situations to be described, aliasing causes an abrupt change in the instantaneous frequency. Compensating for this effect allows for the reconstruction of an unaliased version of the signal.

2.0 TIME-FREQUENCY DISTRIBUTIONS

2.1 INTRODUCTION

The two classical signal representations in signal theory are its time and frequency representations. But as Gabor[13] noted, “both are idealizations...Our everyday experiences - especially our auditory sensations - insist on a description in terms of both time and frequency”.

“The fundamental idea of time-frequency analysis is to describe how the spectral content of a signal changes in time and to develop the physical and mathematical ideas needed to understand what a time-varying spectrum is” [8]. Time-Frequency Distributions (TFD) describe frequency over time, thus providing information about what frequencies existed at each instant of time. TFD is basically a joint distribution which gives the fraction of total energy of the signal at a particular time and frequency. Since TFDs tell as to how much of the total is in a particular time frequency cell, it should be positive for all values of time and frequency.

2.2 CONTINUOUS TFDS

2.2.1 Wigner Distribution

The Wigner Distribution (WD) was introduced by Wigner in 1934 for application in quantum mechanics. It was later recognized as a powerful tool for time-frequency analysis of signals and can be interpreted as a distribution of the signal energy in time and frequency. The WD can be evaluated from both time or the frequency representation of a signal [5].

The WD in terms of the time signal $s(t)$ can be expressed as:

$$W(t, f) = \int_{-\infty}^{+\infty} e^{-j2\pi f\tau} s^*(t - \frac{\tau}{2}) s(t + \frac{\tau}{2}) d\tau \quad (2.1)$$

and in terms of the Fourier transform of $s(t)$, $S(f)$ as:

$$W(t, f) = \int_{-\infty}^{+\infty} e^{-j2\pi t\nu} S^*(f + \frac{\nu}{2}) S(f - \frac{\nu}{2}) d\nu \quad (2.2)$$

$$= \int_{-\infty}^{+\infty} e^{-j2\pi t\nu} S(f + \frac{\nu}{2}) S^*(f - \frac{\nu}{2}) d\nu \quad (2.3)$$

A peculiarity of the WD is that it is not strictly nonnegative, except for a chirp signal. Additionally, for multicomponent signals, that is signals containing more than one part having their own identity in some sense, the WD introduces interference terms. In other words, the WD of sum of two signals is not the same as the sum of the WD of each signal. These interference terms indicate energy in places where one would not expect.

2.2.2 Cohen's General Class of TFDs

In 1966, Cohen gave a unified formulation from which all TFDs can be obtained:

$$\rho(t, f) = \int_{-\infty}^{+\infty} \int_{-\infty}^{+\infty} \int_{-\infty}^{+\infty} e^{j2\pi\nu(u-t)} g(\nu, \tau) s^*(u - \frac{\tau}{2}) s(u + \frac{\tau}{2}) e^{-j2\pi f\tau} d\nu du d\tau \quad (2.4)$$

where $g(\nu, \tau)$ is an arbitrary function, or the kernel. Different distributions can be obtained by taking different kernels. The kernel method has a number of advantages such as [7]:

- It is easy to generate the distributions by just choosing the kernel function. For example, the WD is obtained by $g(\nu, \tau) = 1$.
- The distributions with certain characteristics can be extracted by constraining the kernel
- The properties of an unknown distribution can be easily determined by examining the kernel.

The properties of TFDs can be represented in terms of the kernel function as [6]:

- For the TFD to be real, $g(\nu, \tau) = g^*(-\nu, -\tau)$.

- The energy of the TFD equals the energy of the signal when $g(0,0) = 1$

$$\int \rho(t, f) dt = |S(f)|^2 \quad \text{if } g(0, \tau) = 1$$

$$\int \rho(t, f) df = |s(t)|^2 \quad \text{if } g(\nu, 0) = 1$$

- The first conditional moments of the TFD yield the IF and TD when the following equations are satisfied

$$\frac{\partial g(\nu, \tau)}{\partial \tau} |0, 0 = \frac{\partial g(\nu, \tau)}{\partial \nu} |0, 0 = 0 \quad (2.5)$$

2.2.3 Spectrogram

The short-time frequency transform (STFT), is the main method used for time-frequency analysis, and was first developed for analyzing speech signals [25].

To compute the STFT, the signal, $s(t)$, is divided into small segments which are then fourier transformed. To achieve this a window function, $h(t)$ is used. STFT can be represented as:

$$S(t, f) = \int_{-\infty}^{\infty} s(\tau) h^*(\tau - t) e^{-j2\pi f\tau} d\tau \quad (2.6)$$

The spectrogram is the TFD obtained by taking the magnitude square of the STFT,

$$P_{SP}(t, f) = |S(t, f)|^2$$

The spectrogram is obviously positive but does not give the marginal densities $|s(t)|^2$ and $|S(f)|^2$. Additionally, the window has a significant input on the results obtained. For a given signal one window may be more appropriate than another, thus requiring knowledge about the signal for better analysis. Also in case of a multicomponent signal, each signal component would require its own window for the best results. For such cases, a single window will not be sufficient for signal analysis. Furthermore, as the length of the window is reduced, the time resolution becomes better but the frequency resolution degrades, and vice versa.

The spectrogram can be obtained from Cohen's generalized class of TFDs by taking the kernel to be a WD of the window $h(t)$. Thus, the spectrogram can be represented as a convolution in time and frequency of the WD.

2.3 DISCRETE-TIME TIME FREQUENCY DISTRIBUTION (DTFD)

To enable TFDs to be applicable in discrete-time applications the concept of continuous TFDs need to be transferred to the case of discrete-time signals, thus giving rise to DTFTs. It is desirable that the DTFT should retain as many properties of the TFD as possible.

To understand the DTFT, we consider the discrete-time Wigner distribution in detail.

2.4 DISCRETE-TIME WIGNER DISTRIBUTION (DWD)

Let $s(n)$ and $g(n)$ be two discrete-time signals. Then the cross-Wigner Distribution can be defined as:

$$W_{s,g}(n, \omega) = 2 \sum_{k=-\infty}^{\infty} e^{-j2\omega k} s(n+k) g^*(n-k) \quad (2.7)$$

And the auto-Wigner Distribution can be defined as:

$$W_s(n, \omega) = W_{s,s}(n, \omega) = 2 \sum_{k=-\infty}^{\infty} e^{-j2\omega k} s(n+k) s^*(n-k) \quad (2.8)$$

It is clear that the DWD is a function of n (discrete) and ω (continuous). One of the important properties of the DWD is its Periodicity. As pointed out in [5], the DWD as formulated above is periodic with period π with respect to ω .

$$W_{s,g}(n, \omega) = W_{s,g}(n, \omega + \pi)$$

2.4.1 Relationship between Discrete and Continuous WD

Let the $s_a(t)$ be the continuous-time signals which after sampling results in $s(n)$. Then the sampling relation for DWD can be shown to be as follows [5]:

$$W_s(n, \omega) = \frac{1}{T} \sum_{k=-\infty}^{\infty} W_{s_a}(nT, \frac{\omega + k\pi}{T}) \quad (2.9)$$

where $W_{s_a}(t, \omega)$ is the continuous WD of the signal $s_a(t)$. As we will show, this relationship between the continuous and discrete TFD can be used to identify aliasing in some cases, and correct for it.

A lot of research in aliasing has been done for discrete Wigner distributions (DWD), which when computed traditionally require to be sampled at twice the Nyquist rate to be alias-free. Many have made efforts to obtain alias-free DWDs at Nyquist rate [23, 2, 4, 14, 18]. Costa [9, 10] summarizes and compares these efforts and their results. [4, 19, 21, 1, 15, 20] have given alternative definitions for the DWD. Only the technique given by Nuttall [19] was found to be alias-free for signals sampled at the Nyquist rate. But it requires additional computations.

2.5 INSTANTANEOUS FREQUENCY

In communications, some form of modulation is required since a purely monochromatic signal cannot transmit any information [22]. The most widely used modulation techniques are Amplitude Modulation (AM) and Frequency modulation (FM). FM is a modulation technique in which the instantaneous frequency (IF) is varied in time. As Carson and Fry pointed out in [3], FM was first investigated based on the belief that FM could help reduce the bandwidth requirements for transmission, which was shown otherwise by John Carson in 1922. When radio transmission was introduced the interest in FM was revived. Also FM provided reduced noise-to-signal ratio for the received signal, as compared to AM.

Thus, it was of interest to find out how the parameters of the signal, especially the frequency varied with time. The IF of a complex signal is defined as the derivative of the phase of the signal, i.e. if $z(t)$ is a complex signal expressed as $A(t)e^{j\phi(t)}$, then

$$IF = \frac{d\phi'(t)}{dt} = \omega_i(t) \quad (2.10)$$

But this definition is very ambiguous as there are infinite number of ways for expressing a real signal in a complex form. To overcome this ambiguity and to determine instantaneous APF of AM-FM signals, a number of methods have been developed. A few of these techniques

are discussed briefly in the following sections.

The definition of IF (equation (2.10)) was first given by Carson and Fry [3], in 1937, which was later reinforced by the work of Van der Pol [11]. Carson and Fry, using electric circuit theory concepts tried to generalize frequency by representing it as a function of time. They showed that the IF could be expressed as the derivative of the phase of a complex signal (equation (2.10)). Later, Van der Pol using harmonic motion concepts came up with the same definition of IF, i.e. derivative of the phase of the signal.

But the problem with this definition was that there were infinite number of ways of expressing the real signal in complex form, each giving completely different results for the instantaneous amplitude and phase (thus IF) of the signal. A real signal $x(t)$ can be expressed as $x(t) = \text{Re}\{A(t)e^{j\phi(t)}\}$. There exist an infinite number of pairs $[A(t), \phi(t)]$ whose real part is equal to the signal $x(t)$.

Gabor gave a solution for this ambiguity in 1946 [13]. He proposed the technique of finding the unique complex signal, called the analytic signal (AS), by inverting the fourier transform of the real signal over the positive frequency range only. This procedure is equivalent to taking the imaginary part of the complex signal as the Hilbert transform of the given real part.

Let $x(t)$ be a real signal. The AS of $x(t)$ as proposed by Gabor can be expressed as:

$$z(t) = AS\{x(t)\} = x(t) + j\text{Hilbert}\{x(t)\} \quad (2.11)$$

$$\text{Hilbert}(x) = \frac{1}{t\pi} * x$$

$$Z(\omega) = \begin{cases} 2X(\omega) & \omega > 0 \\ 0 & \omega < 0 \end{cases} \quad (2.12)$$

Thus the IF could be uniquely calculated from the AS as the derivative of the phase of the AS. Vakman [24] showed that only the analytic signal technique satisfies certain physical conditions, Amplitude continuity, harmonic correspondence, phase independence of scaling. However, other properties, such as requiring that the complex representation be bounded in magnitude if the real signal is bounded in magnitude, or requiring $|z(t)| = 0$ for $|t| > T$

if $|x(t)| = 0$ for $|t| > T$, lead to techniques other than the Hilbert transform/ analytic signal [16, 17]

Another technique for obtaining a unique complex signal for a given real signal was introduced by Loughlin and Tacer [17]. This technique uses Cohen's positive time-frequency distribution and the complex signal so obtained satisfies a set of reasonable physical conditions which the AS method failed to satisfy for most of the real signals. The technique proposed that the phase of the complex signal be split into two parts, one corresponding to the FM (ϕ_f) and the other to the AM (ϕ_a). The FM part could be found using the first conditional moment of the positive TFD ($\omega(t)$) as:

$$\phi_f = \int_0^t \omega(\tau) d\tau \quad (2.13)$$

The amplitude and the rest of the phase could be obtained using coherent demodulation. The coherent demodulation gives the "In-Phase AM component" ($A_I(t)$) and the "Quadrature AM component" ($A_Q(t)$), which constitute the complex amplitude $A_I(t) + jA_Q(t) = A(t)e^{j\phi_a(t)}$. Thus the complex signal can then be written as

$$z(t) = A(t)e^{j(\phi_f(t) + \phi_a(t))} \quad (2.14)$$

Another technique for obtaining the IF of a signal is by calculating the first conditional moment of TFDs like Spectrogram, Wigner-Ville distribution, positive Cohen distribution. One of the earliest TFDs was obtained using the Filterbank/ Short-time Fourier Transform (STFT). STFT for a complex signal $z(t)$ can be expressed as

$$y(t, \omega) = \int z(t) h^*(\tau - t) e^{j\omega\tau} d\tau$$

Here, $z(t) = A(t)e^{j\phi(t)}$ and $h(t)$ is the window. Using this equation, the spectrogram can be computed as [8]

$$P_{sp}(t, \omega) = |y(t, \omega)|^2$$

The first conditional moment of the spectrogram can be obtained as:

$$\langle \omega \rangle_t = \frac{\int \omega P_{sp}(t, \omega) d\omega}{\int P_{sp}(t, \omega) d\omega}$$

$$\text{or, } \langle \omega \rangle_t = \frac{\int A^2(\tau) \phi'(\tau) h^2(\tau - t) d\tau}{\int A^2(\tau) h^2(\tau - t) d\tau}$$

It can be shown that as $h(t) \longrightarrow \delta(t)$, i.e. ultra-wide band spectrogram, $\langle \omega \rangle_t \longrightarrow \phi'(t)$

3.0 INTRODUCTION OF THE METHOD TO IDENTIFY POTENTIAL ALIASING, AND COMPENSATE FOR IT

In this chapter, we discuss the underlying principle of aliasing in the time-frequency domain and the proposed method used to identify aliasing and compensate for it.

A few efforts have been made to recover signals sampled at lower rates than the Nyquist rate. Fonte [12] introduces a technique that allows aliased components of a signal to be identified and measured. This has been achieved by changing the sampling rate and comparing the spectra so obtained. This approach requires that one is able to re-sample the continuous-time signal at different rates, and is limited to line spectra. Accordingly, it differs from our approach in that multiple sampling rates are used, and it is limited to signals consisting of tonal components. In contrast, as we will show, our approach utilizes only one sampling frequency – we work directly from the sampled signal obtained at whatever sampling rate was employed – and is limited to FM signals.

We reconstruct the original signal after it has been aliased using time-frequency technique. We used a spectrogram but other methods could be used. The only data available is the aliased form of the signal.

This research addresses aliasing in FM signals. We express the signal in complex form in terms of its amplitude and phase as $x(t) = A(t)e^{j\phi(t)}$. Our approach is restricted to signals which have continuous IF, such that they exhibit a continuous trajectory in the time-frequency plane. Also we assume that the amplitude $A(t)$ is such that in the time-frequency plane, the signal is locally narrowband.

We illustrate the main idea using the discrete-time Wigner distribution (DTWD) of a chirp signal. Let $f(n)$ be a discrete-time sampled chirp,

$$f(n) = Ae^{j\alpha n^2/2}$$

The DTWD for $f(n)$ is thus given by

$$W_f(n, \theta) = |A|^2 \sum_k \delta(\theta - \alpha n - k\pi)$$

Figure (3.1) shows the DTWD for $f(n)$ when it has been sampled at the correct sampling rate, i.e. at a rate more than twice the Nyquist rate for the signal. It is seen that the window displays the DTWD (unaliaised) as one would expect to see.

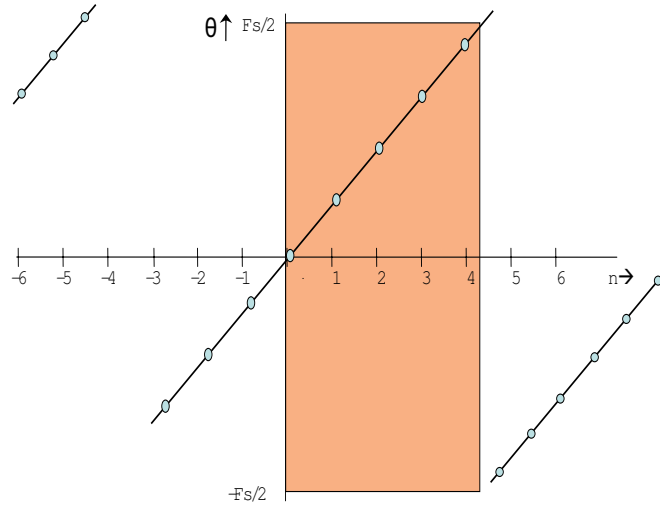


Figure 3.1: *Unaliased WD of Chirp Signal. Gray region represents the observed range of the DTWD*

Under conditions when $f(n)$ has been sampled at a rate lower than twice the Nyquist rate, DTWD shows aliasing effects. One such case has been shown in the figure (3.2). If only the shaded area is considered, which represents the region over which we observed (i.e. sampled) the signal, it can be seen that the aliasing causes the IF of the signal to jump by 2π . Thus the original signal can be reconstructed from its aliased version by correcting for the 2π - jumps in the IF/ phase of the signal.

This motivated us to explore the effects of aliasing on DTFDs in depth and to develop a technique to recover the complex signal when only its aliased version available. But this behavior -jumping by 2π - is true only for complex signals, which greatly restricts the applications of this method. Keeping this in mind, we explored the aliasing effects on real

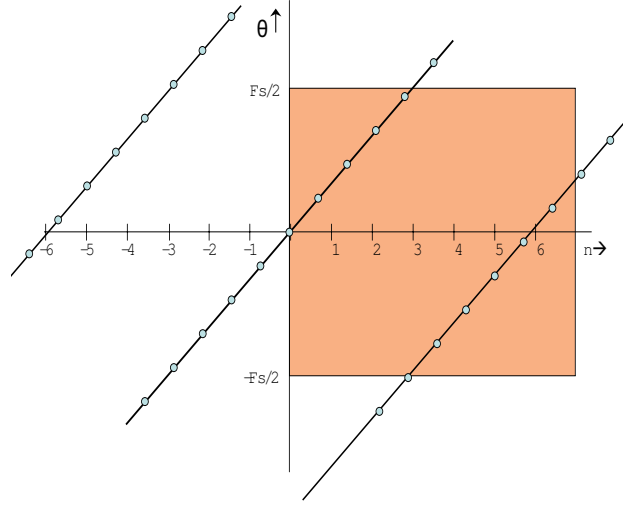


Figure 3.2: *Aliased WD of Chirp Signal (Exponential). Now over the time interval that we observed the signal (gray region), we see a sudden discontinuity in the trajectory when the IF greater than $F_s/2$.*

signals, to find a similar trend due to aliasing. Let $x(n) = \text{Re}\{f(n)\} = A\cos(\alpha n^2/2)$. The DTWD is shown in figure (3.3).

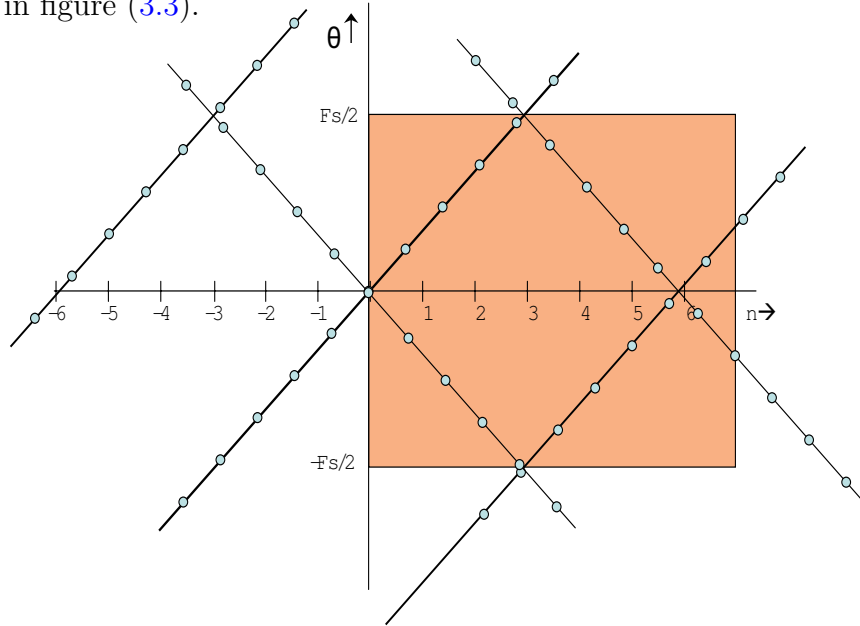


Figure 3.3: *Aliased WD of Chirp Signal (Real)*

Here again if only the shaded region is considered (representing the interval over which

the original signal was sampled), it can be seen that a trend exists depending on the amount of aliasing. The signal goes till the maximum, i.e., $\frac{F_s}{2}$ and then turns (slope changes from positive to negative) and continues till it reaches the minimum $-\frac{F_s}{2}$ and then turns again (slope changes from negative to positive). The signal being bounded by $[-\frac{F_s}{2}, \frac{F_s}{2}]$, turns every time it reaches the boundary. Thus, it seems possible to recover the signal from the aliased version if the turns could be appropriately corrected (continuously increasing slope).

To simplify the procedure, the analytic signal (AS) corresponding to $x(n)$ was obtained, $y(n) = \text{Analytic}[x(n)] = Ae^{j\phi(n)}$. The DTWD obtained for $y(n)$ is shown in figure (3.4). Here only the turns in the positive region can be seen. Now the signal is bounded by $[0, \frac{F_s}{2}]$.

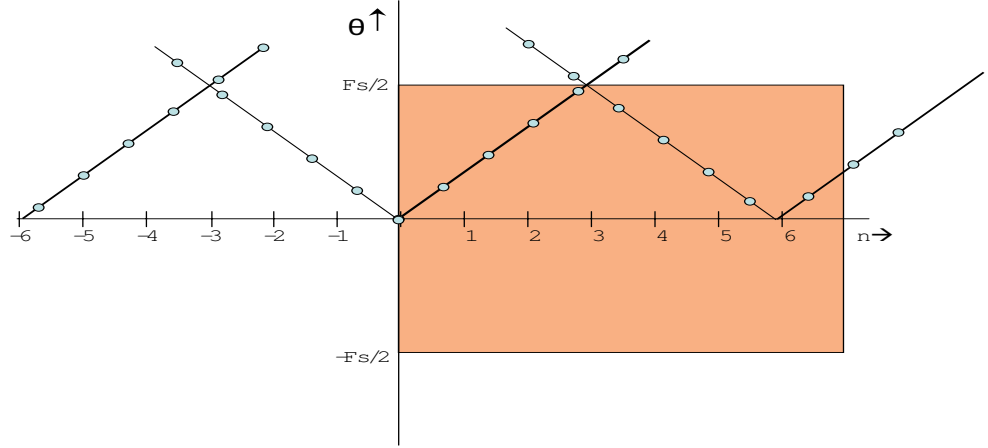


Figure 3.4: *Aliased WD of Chirp Signal (Analytic)*

The considerations above suggest that, for certain signals, it is possible to identify when aliasing has occurred by observing the signal in the time-frequency plane. Further, given how aliasing is manifest in the plane - as sudden changes in the trajectory of the IF when it exceeds $|\frac{F_s}{2}|$ - it should be possible to correct the IF and reconstruct an unaliased version of the signal.

We describe the proposed method next, and illustrate its utility by several examples. We then consider in more detail the conditions on the signal such that the proposed method will allow for aliasing to be identified and compensated.

3.1 ILLUSTRATION OF THE METHOD

Figure (3.6) shows the block diagram of the method and outlines the steps followed. We used the spectrogram as the TFD to identify aliasing and obtain IF estimates to compensate for the sudden changes in IF due to aliasing. The source code was written using MATLAB, and the MATLAB functions are included in this thesis. The steps are explained below and are illustrated using an example,

$$x(t) = \cos(2\pi 3t^2)$$

Figures(3.5(a) and (b)) show the time-series and the log-spectrogram of the aliased sampled signal $x[n]$.

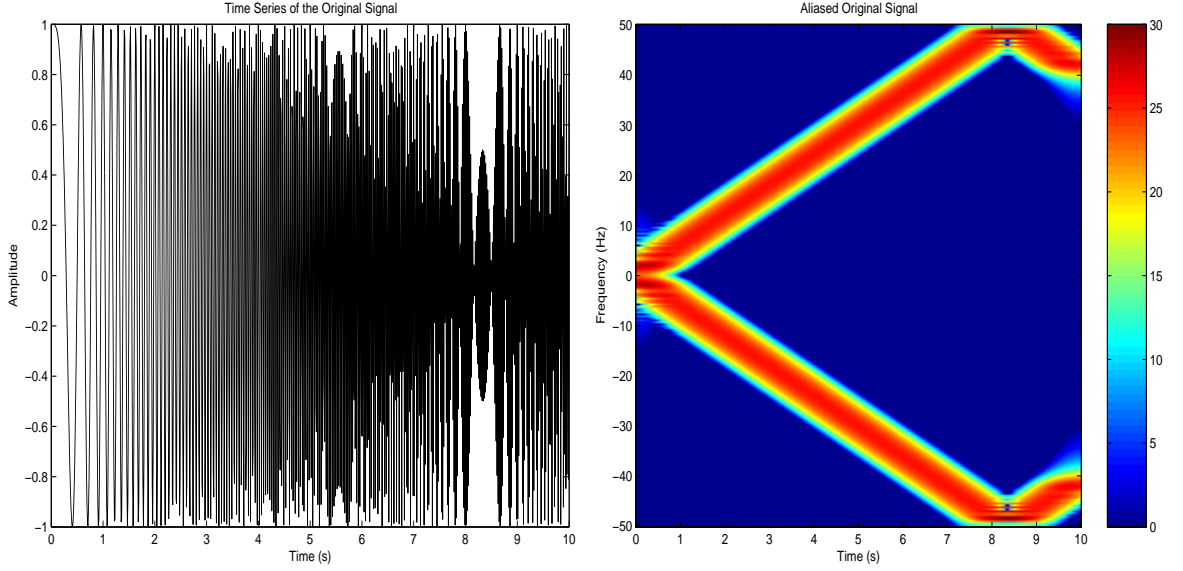


Figure 3.5: (a) Time-series and (b) Log-magnitude spectrogram of the aliased signal

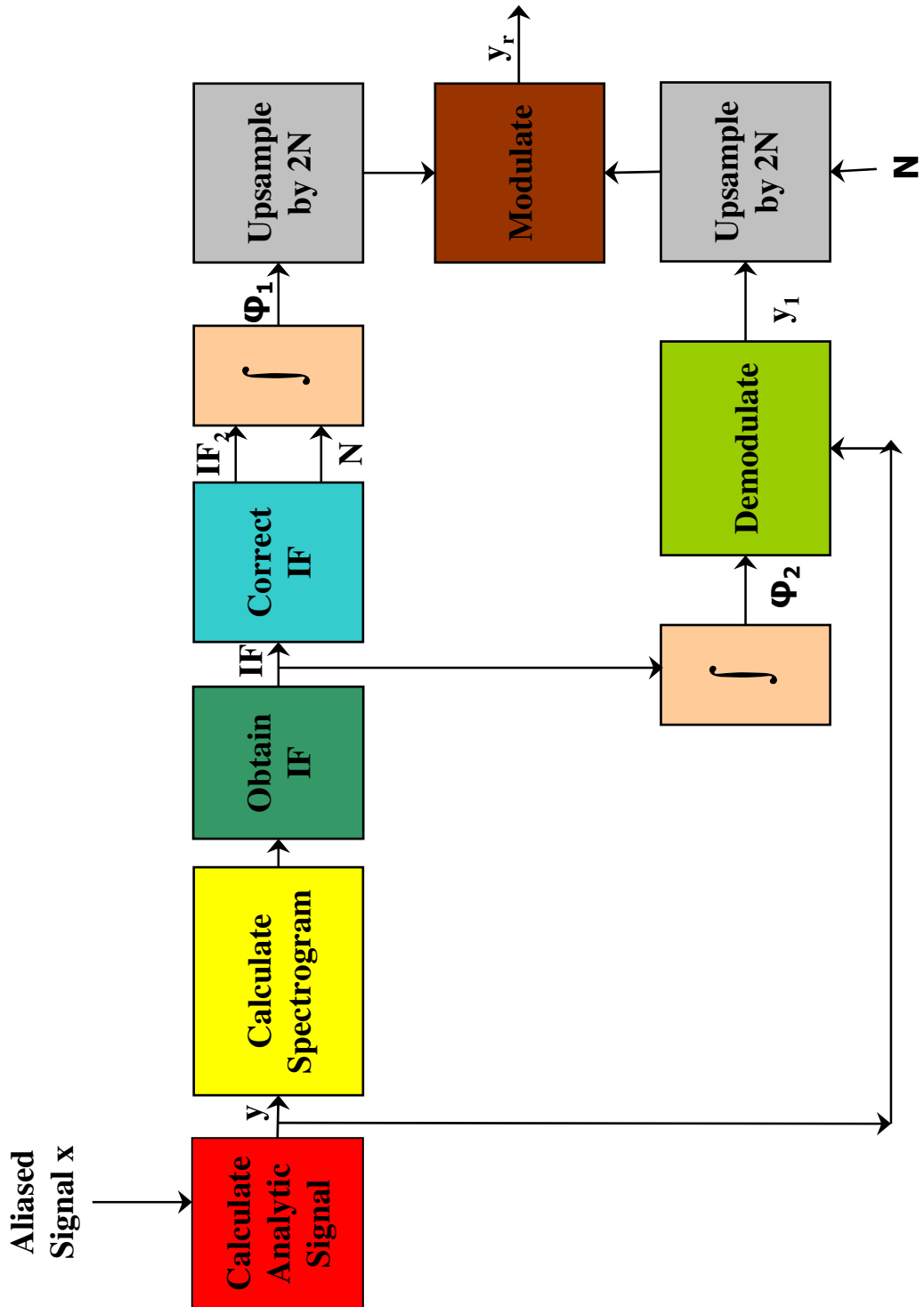


Figure 3.6: Block diagram of a method to compensate for aliasing

3.1.1 Step 1: Analytic Signal

The first step involves the calculation of the AS for a given real signal ($x[n]$). As discussed in chapter, the Analytic Signal can be obtained as

$$y[n] = \text{Analytic}\{x[n]\} = x[n] + j\text{Hilbert}\{x[n]\} = A[n]e^{j\phi[n]}$$

The MATLAB function *hilbert* was used to obtain the analytic signal.

```
y = hilbert(x);      % Calculates the Analytic Signal for the Real Signal x(t)
```

3.1.2 Step 2: Spectrogram

We used the custom function *sgram2* to calculate the spectrogram. One reason for this was that while working on the complex signals, we required to view negative frequencies, which is not possible using the MATLAB function *specgram*. Figure (3.7) displays the spectrogram of the analytic signal $y[n]$.

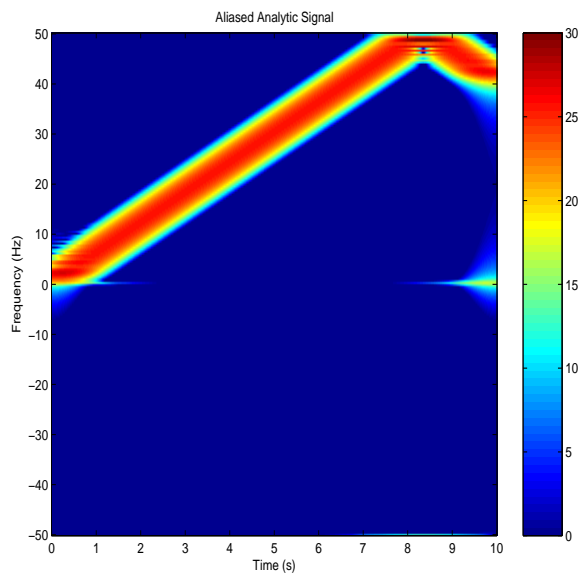


Figure 3.7: *Log-Magnitude Spectrogram of the Analytic Signal $y[n]$*

sgram2 calculates the spectrogram of a signal and returns a 2-sided spectrum $[-\pi, \pi]$, in normalized frequency units. It provides the option of the parameters: *nflen*, number of fft points; *winlen*, Odd length of Hanning window; *shift*, number of samples to shift the window by. The following code shows the usage of *sgram2* and also includes the commands to display the spectrogram so obtained.

```
sg = sgram2(y,256,255,1);           % flen:256, winlen:255, shift:1
[T,F] = size(sg);                   % creates time and frequency vectors
T = 0 : T-1; F = 0 : F-1;
T = T*t(length(t))/T(length(T));   % converts from samples to seconds,
                                     % t:time vector for x(t)
m = 2*pi/(F(length(F))-F(1));       % Fs: sampling rate
b = -pi-m*F(1);                     % converts from bins to samples
F = m*F+b; figure; imagesc(T,F,10*log10(sg')); axis xy;
```

3.1.3 Step 3: Instantaneous Frequency

There are number of ways of obtaining the IF estimates from the TFD, and we have used the peak picking method to obtain the same. For every time instant, the frequency value corresponding to the maximum value of the TFD at that point is obtained. For a monocomponent signal with slowly varying amplitude, the results obtained by peak picking match very closely with the expected values. Before getting the values, the frequency vector was converted into the normalized units (to see variations with $[-\pi, \pi]$ clearly). The following code was used to obtain the IF vector and figure (3.8) displays the estimated IF.

```
IF_o = [];                           % initializes the IF vector
[A,k] = max(sg');                     % returns the indices of the
                                     % maximum values, A,in vector k
for i = 1:1:length(k)
    IF_o = [IF_o F(k(i))];
end;
```

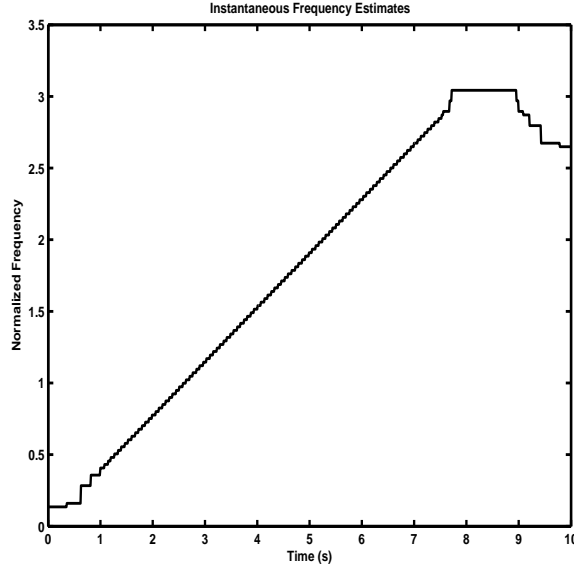


Figure 3.8: *Original IF Estimates for the Analytic Signal $y[n]$*

3.1.4 Step 4: Instantaneous Frequency Correction

The IF estimates for the unaliased version can be obtained from the IF estimates of the aliased signal by correcting the turns in the IF.

Here, IF_c denotes the corrected IF estimates obtained by correcting turns in the original IF_o . And, n is the number of times the signal turns at the boundaries. The Figure (3.9) shows the corrected IF estimates obtained for $y(t)$.

```

IF1 = IF_o;                                % create copies of IF
n = 0;                                     % initialize number of turns
[c,1] = max(IF1); p = find(IF1<max(IF1)); m = find(p>1); while(m)
    n = n+1;
    IF = IF1;
    [A,i] = max(IF_o);
    i = find(IF_o==A);
    IF1 = IF_o(1:min(i)-1);
    k = min(i);
    Value = (n*Fs/2-IF_o(min(i)-1))/((max(i)+min(i))/2-((min(i))))
    IF2 = [IF2 IF_o(max(i)+2:length(IF_o))];

```

```

k = min(i);
while k <= max(i)+1 & k <= length(IF_o)
    IF1=[IF1 IF1(k-1)+Value];          % Correcting Turn
    k = k+1;
end;
IF1 = [IF1 (n*Fs/2-IF_o(max(i)+2:length(IF_o))+n*Fs/2)];
[c,l] = max(IF1);
p = find(IF1<max(IF1));
m = find(p>1);
end;
IF_c = IF1;                                % Corrected IF

```

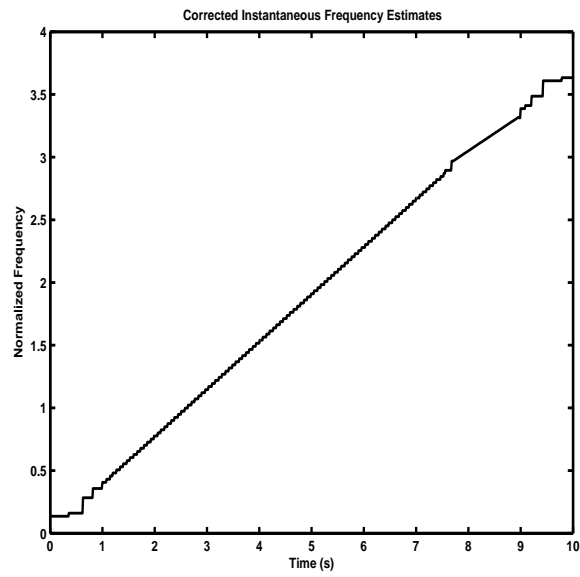


Figure 3.9: *Corrected IF Estimates for the Analytic Signal $y(t)$*

3.1.5 Step 5: Phase Estimation

As mentioned above, the first derivative of the phase of the spectrogram gives the IF. Thus, the phase can be obtained by integrating the IF estimates (obtained in Steps 3 and 4).

$$\begin{aligned}d\phi(t)/dt &= IF \\ \hat{\phi}(t) &= \int IF_o \\ \hat{\hat{\phi}}(t) &= \int IF_c\end{aligned}$$

The MATLAB function `cumsum` was used to calculate the phase. The function `cumtrapz(t,IF)` computes the cumulative sum of IF.

```
Phi_Hat = cumsum(IF_o); Phi_Hat_Hat = cumsum(IF_c);
```

Figures(3.10 (a) and (b)) show the phase estimated for the original and the corrected IF estimates respectively.

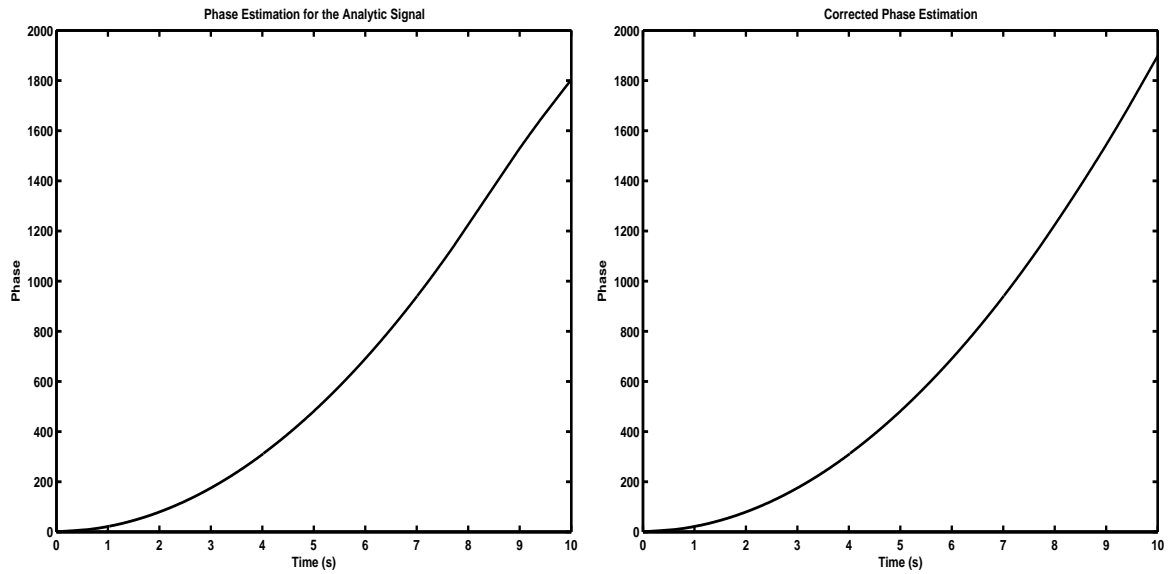


Figure 3.10: *Phase Estimates for the (a) original and (b) corrected IF estimates*

3.1.6 Step 6: Demodulation

The phase estimation obtained from Step 5, was used to demodulate the analytic signal $y[n]$.

Demodulation involves multiplying $y[n]$ with the signal having negative estimated phase $\hat{\phi}(t)$

$$y[n] = A[n]e^{j\phi[n]}$$

Demodulation :

$$\begin{aligned} y_d[n] &= y[n] * e^{-j\hat{\phi}[n]} \\ &= A[n]e^{j\phi[n]} * e^{-j\hat{\phi}[n]} \\ &\approx A(t) \end{aligned} \tag{3.1}$$

In this step we hope to obtain a result which is almost equal to the amplitude of the AS $y[n]$. Figure (3.11) displays the demodulated signal obtained for $y[n]$.

```
y1 = exp(-j*Phi_Hat); y_d = y.*y1;
```

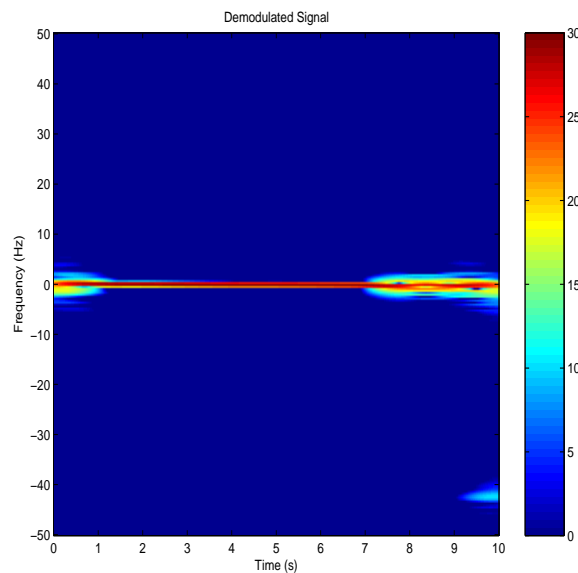


Figure 3.11: *Demodulated Signal*

3.1.7 Step 7: Upsampling

The aliasing problem occurred due to the sampling rate being lower than the required minimum rate (twice the Nyquist Rate for DTFD). Thus the signals need to be corrected and upsampled by the appropriate amount. The demodulated signal (from step 6) and the corrected phase (from step 5) thus need to be upsampled by twice the number of times the signal turns (from step 4). A custom interpolation function *interpolate* was used to upsample the signals.

```
% Upsampling by 2*n
Phi_Corrected = interpolate(Phi_Hat_Hat,n); % upsample corrected phase
y_d_u = interpolate(y_d,n);                % upsample demod. signal
```

The upsampled phase and demodulated signal have been shown in figures (3.12(a), (b)).

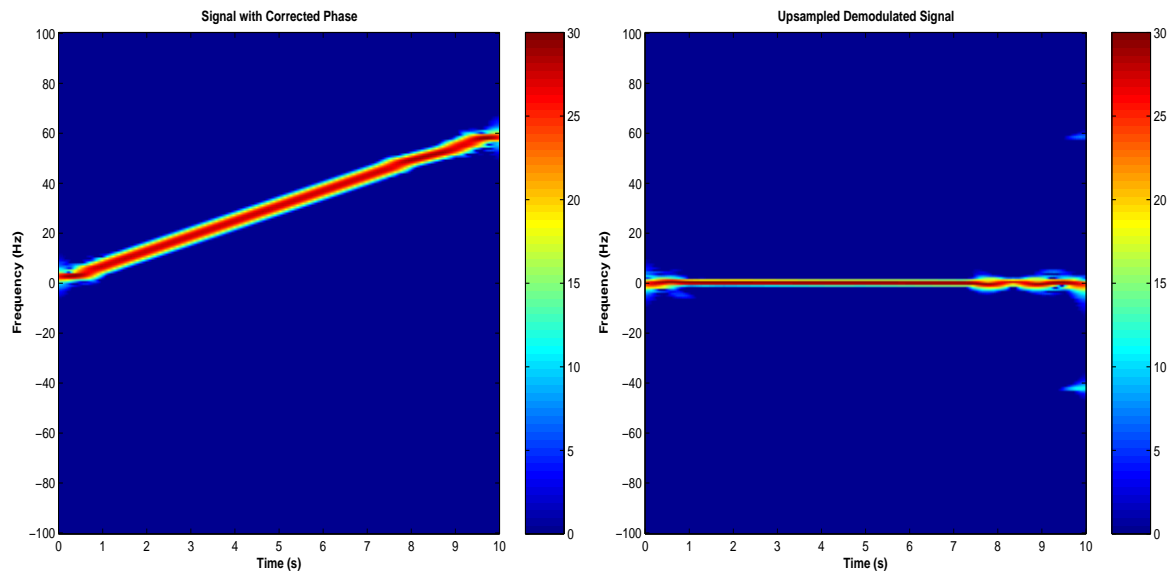


Figure 3.12: (a) Phase signal with upsampled corrected phase and (b) upsampled demodulated signal

3.1.8 Step 8: Reconstruction

This step involves combining the upsampled demodulated signal with the corrected phase ($\hat{\phi}$ from Step 7) to obtain an unaliased version of the original AS $y[n]$.

$$y_r = y_{d_u} \cdot \exp(j \cdot \text{Phi_Corrected});$$

The restored signal obtained for the aliased analytic signal ($y[n]$) in figure (3.5) is shown in figure (3.13).

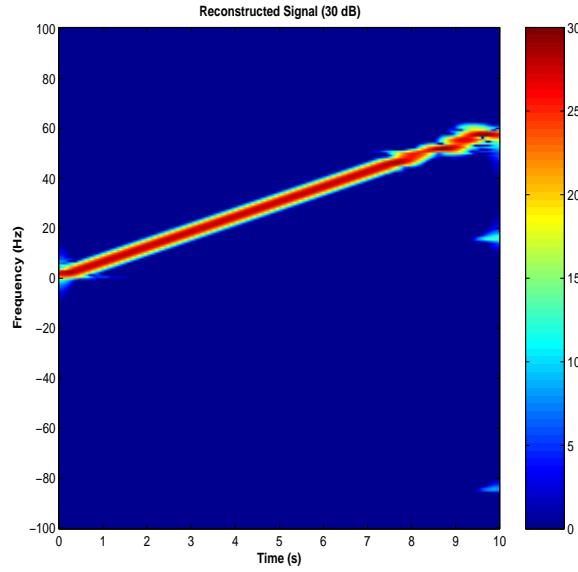


Figure 3.13: *Reconstructed signal*

In the next chapter, we consider sources of error, additional signals, and “best-case” performance given ideal estimates of the IF.

4.0 RESULTS AND DISCUSSION

In this section, we consider ideal estimates of the IF to examine “best-case” performance of the method. We also define the class of signals for which our method is applicable in terms of concentration along the IF for a Wigner distribution of the signal. We consider the Wigner distribution (WD) since it simplifies the derivations and the spectrogram can be considered as a “smoothed” version of the WD.

The WD for a continuous-time signal $s(t)$ is defined as:

$$W_s(t, \omega) = \frac{1}{2\pi} \int s\left(t + \frac{\tau}{2}\right) s^*\left(t - \frac{\tau}{2}\right) e^{-j\omega\tau} d\tau \quad (4.1)$$

Let $s(t) = A(t)e^{j\phi(t)}$, where $A(t)$ specifies the instantaneous amplitude and $\phi(t)$ the instantaneous phase. Substituting this in equation(4.1), we obtain,

$$W_s(t, \omega) = \frac{1}{2\pi} \int A\left(t + \frac{\tau}{2}\right) e^{j\phi\left(t + \frac{\tau}{2}\right)} A^*\left(t - \frac{\tau}{2}\right) e^{j\phi\left(t - \frac{\tau}{2}\right)} e^{-j\omega\tau} d\tau \quad (4.2)$$

$$= \frac{1}{2\pi} \int A\left(t + \frac{\tau}{2}\right) A\left(t - \frac{\tau}{2}\right) e^{j\phi\left(t + \frac{\tau}{2}\right)} e^{j\phi\left(t - \frac{\tau}{2}\right)} e^{-j\omega\tau} d\tau \quad (4.3)$$

since $A(t)$ is real.

Using Taylor Series Expansion of the phase, we have

$$\phi\left(t + \frac{\tau}{2}\right) = \phi(t) + \frac{\tau}{2}\phi'(t) + \frac{\tau^2}{2 * 4}\phi''(t) + \dots$$

and,

$$\phi\left(t - \frac{\tau}{2}\right) = \phi(t) - \frac{\tau}{2}\phi'(t) + \frac{\tau^2}{2 * 4}\phi''(t) - \dots$$

Ignoring terms higher than $\phi'''(t)$, we get

$$\phi(t + \frac{\tau}{2}) - \phi(t - \frac{\tau}{2}) \approx \tau \phi'(t)$$

Substituting this value in equation(4.3) we get,

$$W_s(t, \omega) \approx \frac{1}{2\pi} \int A(t + \frac{\tau}{2}) A(t - \frac{\tau}{2}) e^{j\tau \phi'(t)} e^{-j\omega \tau} d\tau \quad (4.4)$$

Assuming that $A(t)$ remains relatively constant, i.e. for pure FM signals the above equation reduces to:

$$W_s(t, \omega) = A^2(t) \frac{1}{2\pi} \int e^{j\tau \phi'(t)} e^{-j\omega \tau} d\tau \quad (4.5)$$

Using Fourier Transform, we obtain

$$W_s(t, \omega) = A^2(t) \delta(\omega - \phi'(t)) \quad (4.6)$$

Thus, the distribution is centered around the IF for signals where $A(t) \approx \text{constant}$ and $\phi^{(n)}(t) = 0, n \geq 4$. For such cases, the phase calculations using the IF estimates generate results with negligible errors.

Other approximations: Let $-\alpha(t) = \log(A(t))$. Then $s(t) = e^{-\alpha(t) + j\phi(t)}$ and

$$W_s(t, \omega) = \frac{1}{2\pi} \int A(t + \frac{\tau}{2}) A(t - \frac{\tau}{2}) e^{j(\phi(t + \frac{\tau}{2}) + \phi(t - \frac{\tau}{2}))} e^{-j\omega \tau} d\tau \quad (4.7)$$

$$= \frac{1}{2\pi} \int e^{-\alpha(t + \frac{\tau}{2})} e^{-\alpha(t - \frac{\tau}{2})} e^{j(\phi(t + \frac{\tau}{2}) + \phi(t - \frac{\tau}{2}))} e^{-j\omega \tau} d\tau \quad (4.8)$$

Again using Taylor Series,

$$\alpha(t + \frac{\tau}{2}) = \alpha(t) + \frac{\tau}{2} \alpha'(t) + \frac{\tau^2}{2 * 4} \alpha''(t) + \dots$$

and,

$$\alpha(t - \frac{\tau}{2}) = \alpha(t) - \frac{\tau}{2}\alpha'(t) + \frac{\tau^2}{2 \cdot 4}\alpha''(t) + \dots$$

Ignoring higher terms and adding the two equations,

$$\alpha(t + \frac{\tau}{2}) + \alpha(t - \frac{\tau}{2}) \approx 2\alpha(t) + \frac{\tau^2}{4}\alpha''(t)$$

Substituting in equation (4.8), we obtain,

$$W_s(t, \omega) \approx \frac{1}{2\pi} \int e^{-2\alpha(t) - \frac{\tau^2}{4}\alpha''(t)} e^{j\tau\phi'(t)} e^{-j\omega\tau} d\tau \quad (4.9)$$

$$= \frac{1}{2\pi} \int e^{2\log(A(t))} e^{-\frac{\tau^2}{4}\alpha''(t)} e^{j\tau\phi'(t)} e^{-j\omega\tau} d\tau \quad (4.10)$$

Taking the Fourier transform we obtain:

$$\begin{aligned} W_s(t, \omega) &\approx \frac{1}{2\pi} A^2(t) \frac{2\sqrt{\pi}}{\sqrt{\alpha''(t)}} e^{(\frac{2\omega\phi'(t) - \phi'^2(t) - \omega^2(t)}{\alpha''(t)})} \\ &= \frac{A^2(t)}{\sqrt{\pi\alpha''(t)}} e^{(-\frac{(\omega - \phi'(t))^2}{\alpha''(t)})} \end{aligned} \quad (4.11)$$

$\alpha(t) = -\log(A(t))$, Therefore,

$$\alpha'(t) = \frac{-A'(t)}{A(t)}$$

and

$$\begin{aligned} \alpha''(t) &= \frac{-A''(t)}{A(t)} + \frac{(A'(t))^2}{(A(t))^2} \\ &= \frac{A'(t)^2}{A(t)^2} - \frac{A''(t)}{A(t)} \end{aligned}$$

Let $2\sigma_\omega^2(t) = ((\frac{A'(t)}{A(t)})^2 - \frac{A''(t)}{A(t)})$, which we note is the instantaneous bandwidth of the Wigner distribution. Substituting this value in (4.11),

$$W_s(t, \omega) \approx \frac{A^2(t)}{\sqrt{2\pi\sigma_\omega^2(t)}} e^{(-\frac{(\omega - \phi'(t))^2}{2\sigma_\omega^2(t)})} \quad (4.12)$$

If $A(t)$ is relatively constant equation(4.12) becomes the same as (4.6). But if $A(t)$ changes with time we obtain a Gaussian function centered around the instantaneous frequency. The more slowly varying is $A(t)$, the better the concentration along the IF

4.1 IDEAL CASES

To further illustrate the method and to prove that given ideal IF estimates the method recovers the restored signal almost perfectly (based on numerical simulations) for the class of signals having moderate AM and continuous FM and where the TFD follows the IF (equation 4.12) we provide a few examples.

1. Chirp with Constant Amplitude (figures 4.1, 4.2)
2. Chirp with Gaussian amplitude (figures 4.3, 4.4)
3. Chirp with Sinusoidal amplitude (figures 4.5, 4.6)

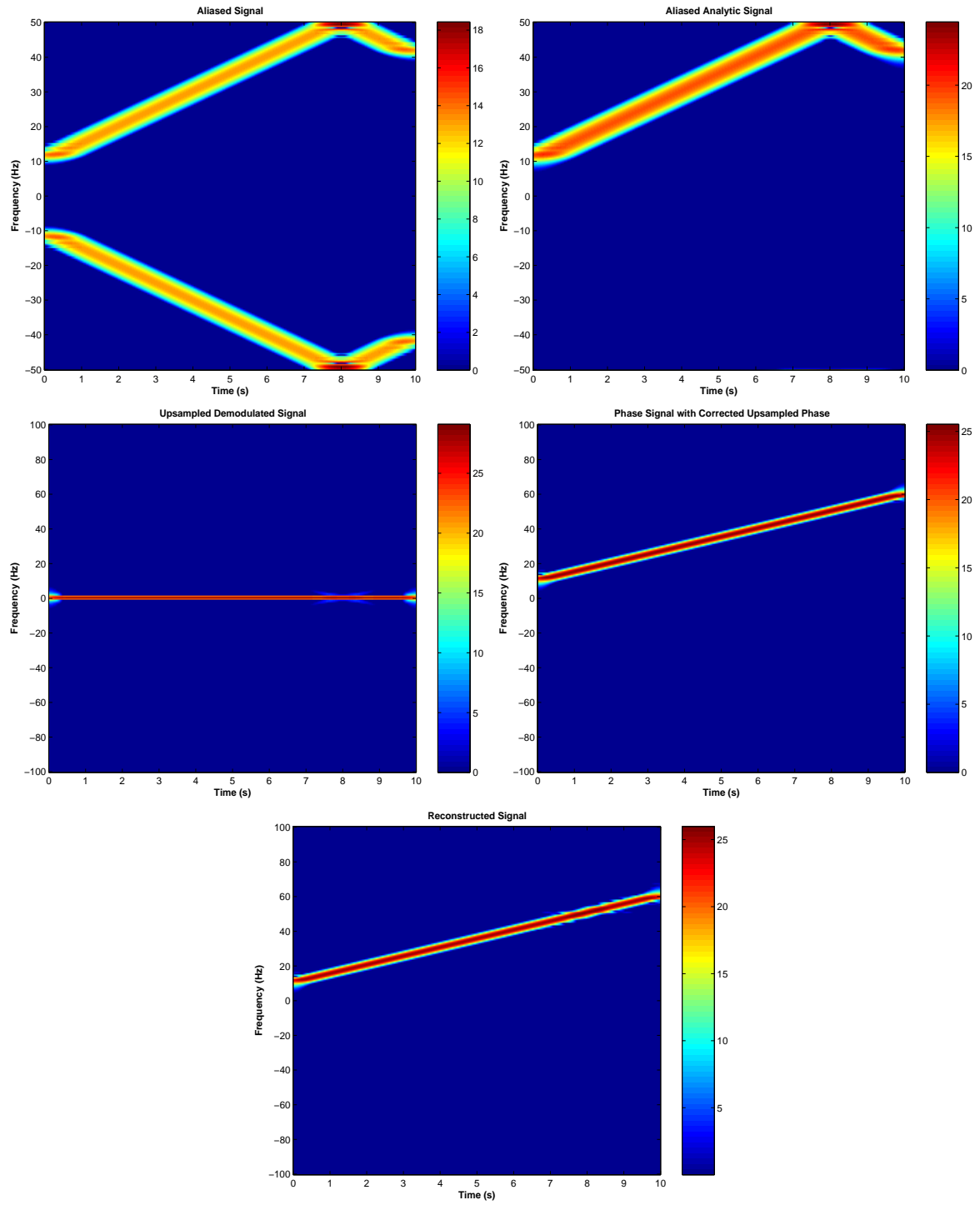


Figure 4.1: *Ideal Case 1: Constant Amplitude, Log-magnitude spectrogram of (a) the aliased signal, (b) the analytic signal, (c) upsampled demodulated signal, (d) phase signal with corrected phase and (e) reconstructed signal*

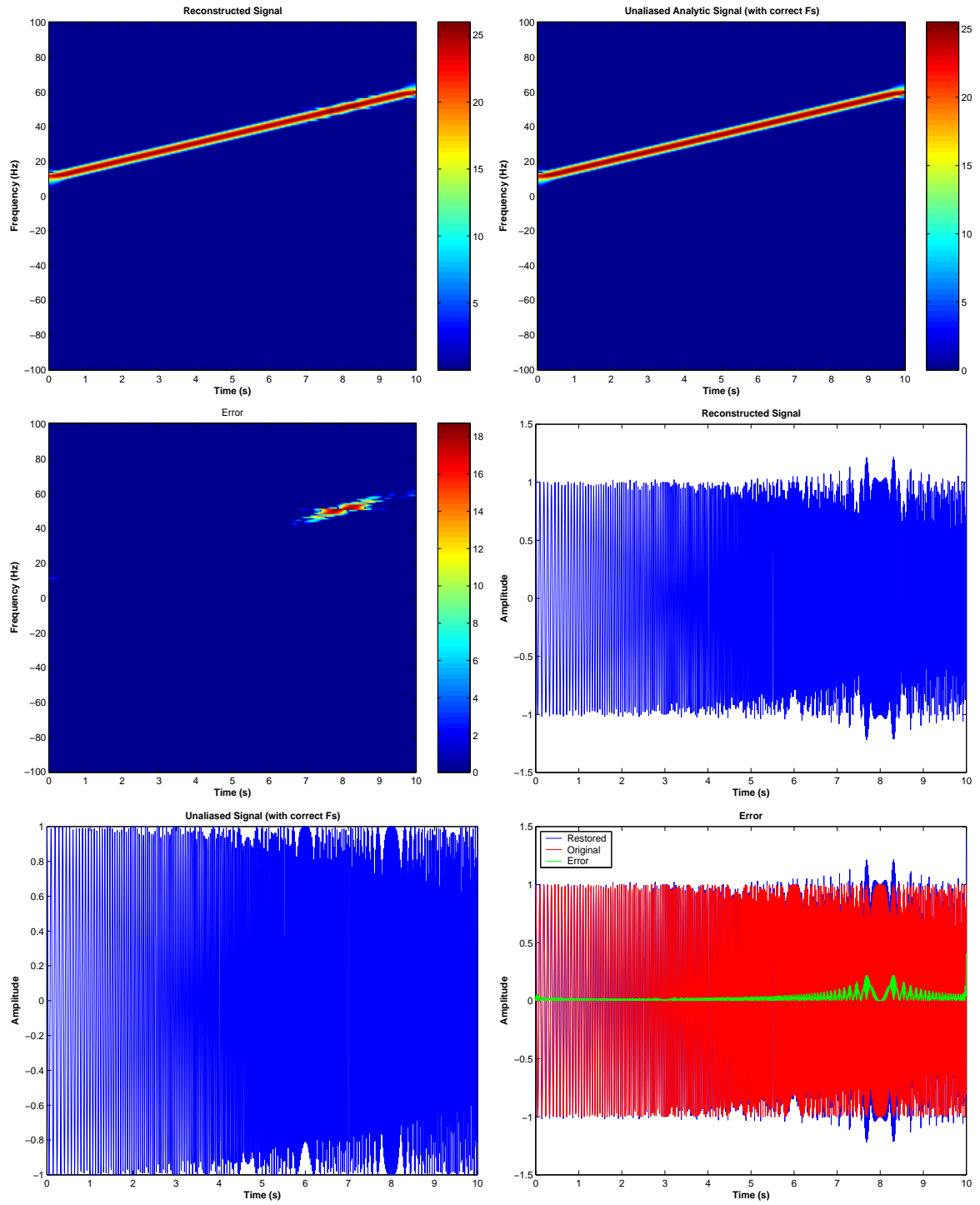


Figure 4.2: *Ideal Case 1: Constant Amplitude, (a) Log-magnitude spectrogram of the restored signal (b) log-magnitude spectrogram of the “true” unaliased signal (with correct sampling rate) (c) error between (a) and (b). Time-series of the (d) reconstructed signal, (e) “true” unaliased signal (with correct sampling rate) and (f) the error between (d) and (e)*

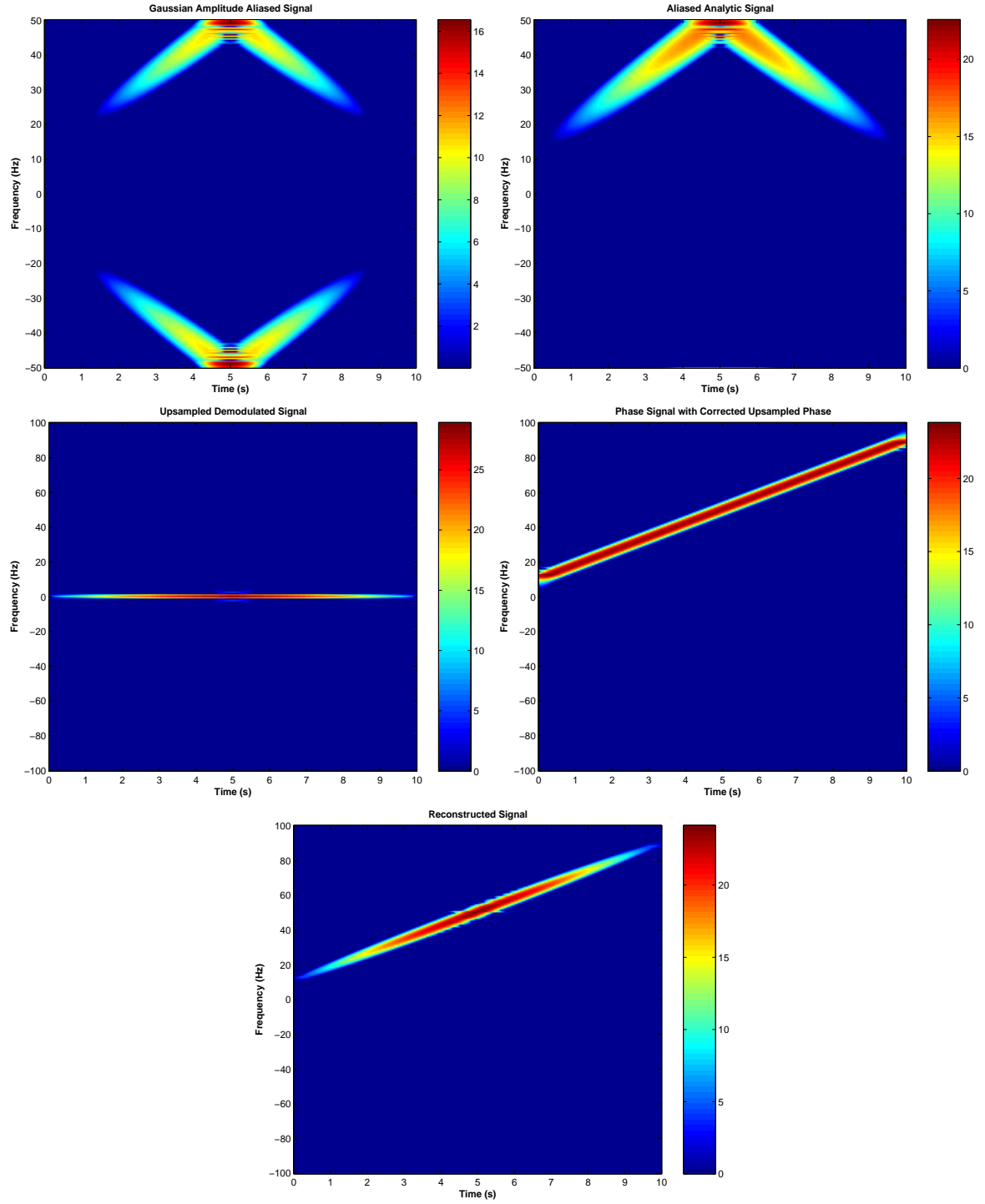


Figure 4.3: *Ideal Case 2: Gaussian Amplitude, Log-magnitude spectrogram of (a) the aliased signal, (b) the analytic signal, (c) upsampled demodulated signal, (d) phase signal with corrected phase and (e) reconstructed signal*

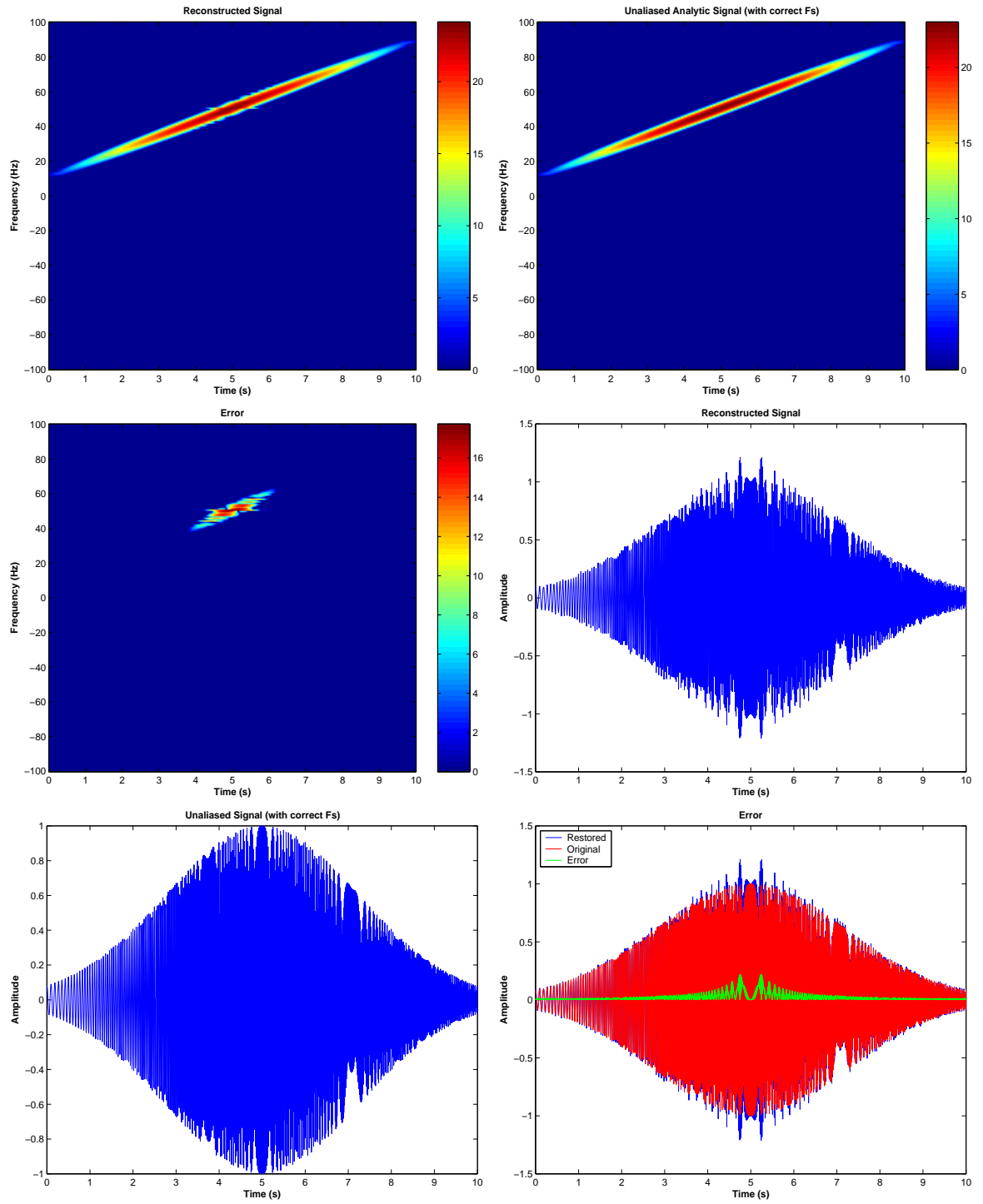


Figure 4.4: *Ideal Case 2: Gaussian Amplitude, (a) Log-magnitude spectrogram of the restored signal (b) log-magnitude spectrogram of the “true” unaliased signal (with correct sampling rate) (c) error between (a) and (b). Time-series of the (d) reconstructed signal, (e) “true” unaliased signal (with correct sampling rate) and (f) the error between (d) and (e)*

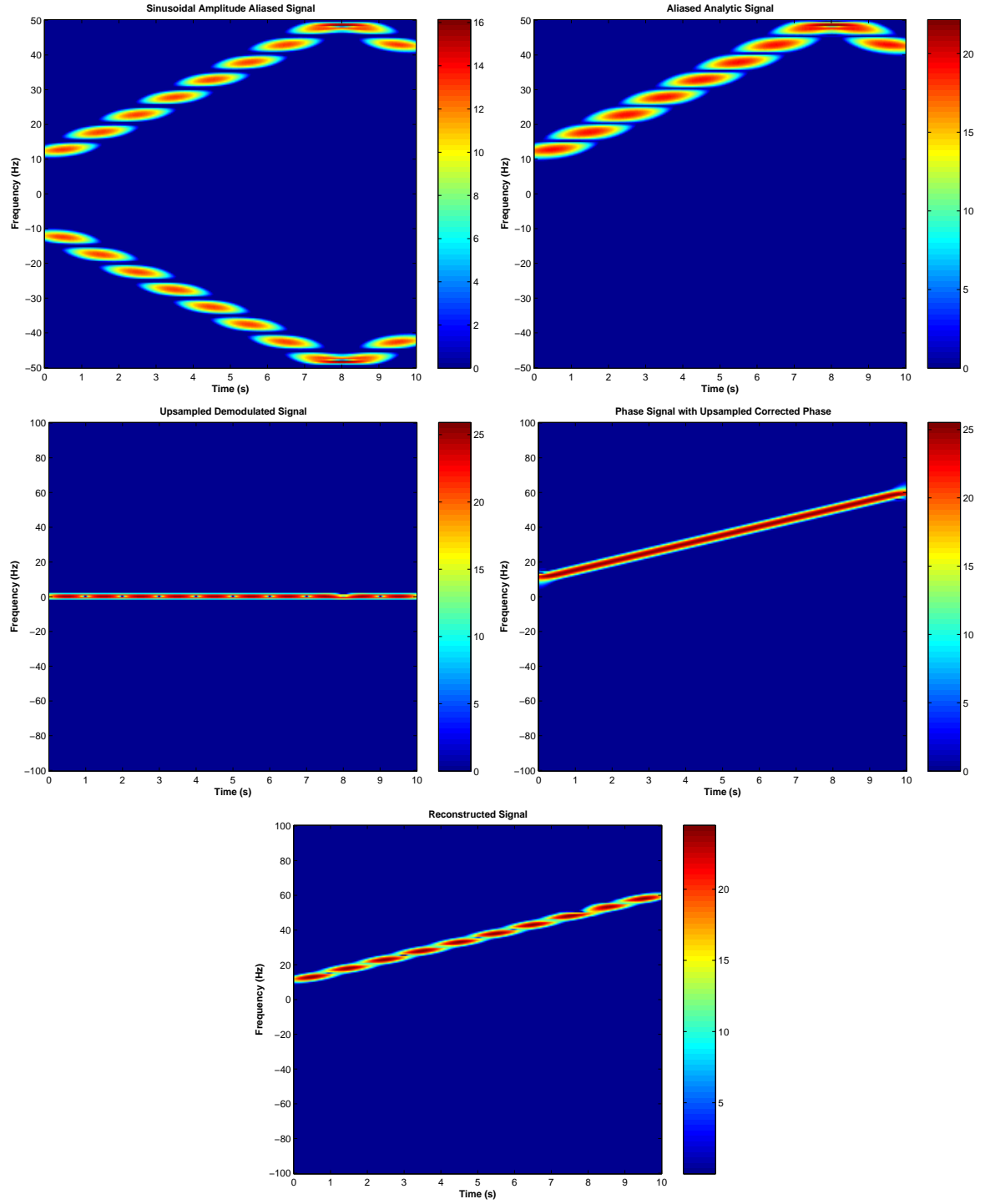


Figure 4.5: *Ideal Case 3: Sinusoidal Amplitude, Log-magnitude spectrogram of (a) the aliased signal, (b) the analytic signal, (c) upsampled demodulated signal, (d) phase signal with corrected phase and (e) reconstructed signal*

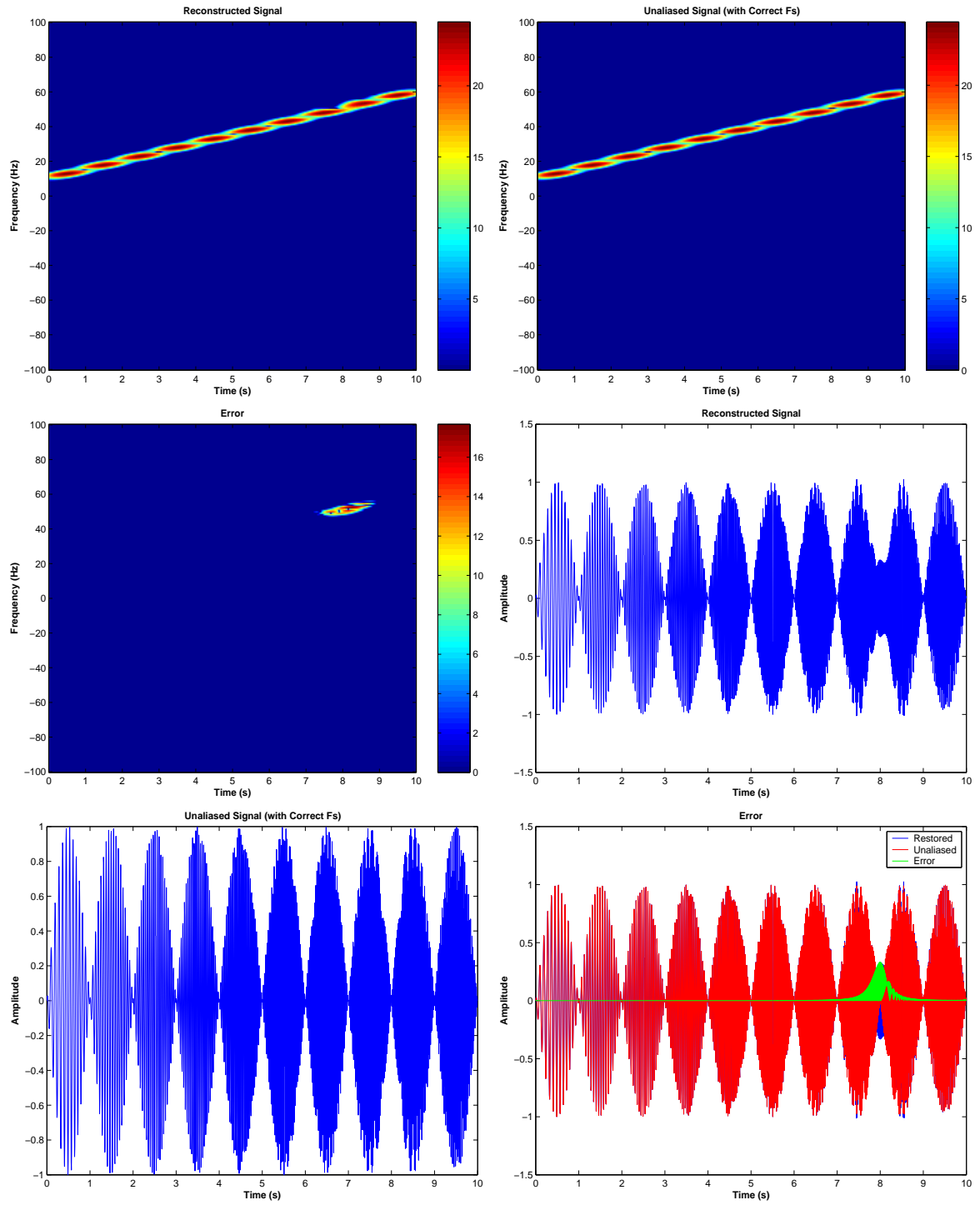


Figure 4.6: *Ideal Case 3: Sinusoidal Amplitude*, (a) Log-magnitude spectrogram of the restored signal (b) log-magnitude spectrogram of the “true” unaliased signal (with correct sampling rate) (c) error between (a) and (b). Time-series of the (d) reconstructed signal, (e) “true” unaliased signal (with correct sampling rate) and (f) the error between (d) and (e)

4.2 NON-IDEAL CASES

We can see from these simulations that the magnitude of the error increases as the amplitude deviates from the constant amplitude condition, and varies with time.

The technique was implemented on various signals shown on the following pages. These include:

1. Chirp with Gaussian amplitude (figure [4.7](#))
2. Chirp with Sinusoidal amplitude (figure [4.8](#))
3. Chirp with amplitude as a combination of sinusoids (figure [4.9](#))
4. Signal with cubic phase (figure [4.10](#))
5. Chirp with constant amplitude and multiple turns in aliasing (figure [4.11](#))

4.3 A FEW LIMITATIONS

A couple of examples where this technique is limited:

- Signal which is comprised of number of tones which jump, i.e. when the signal does not have continuous trajectory (figure [4.12](#))
- Signal which inherently has increasing slope till $\frac{Fs}{2}$ and then decreasing, without actual aliasing taking place. In such a case, the technique will wrongly identify the signal to be aliased and will try to correct it.

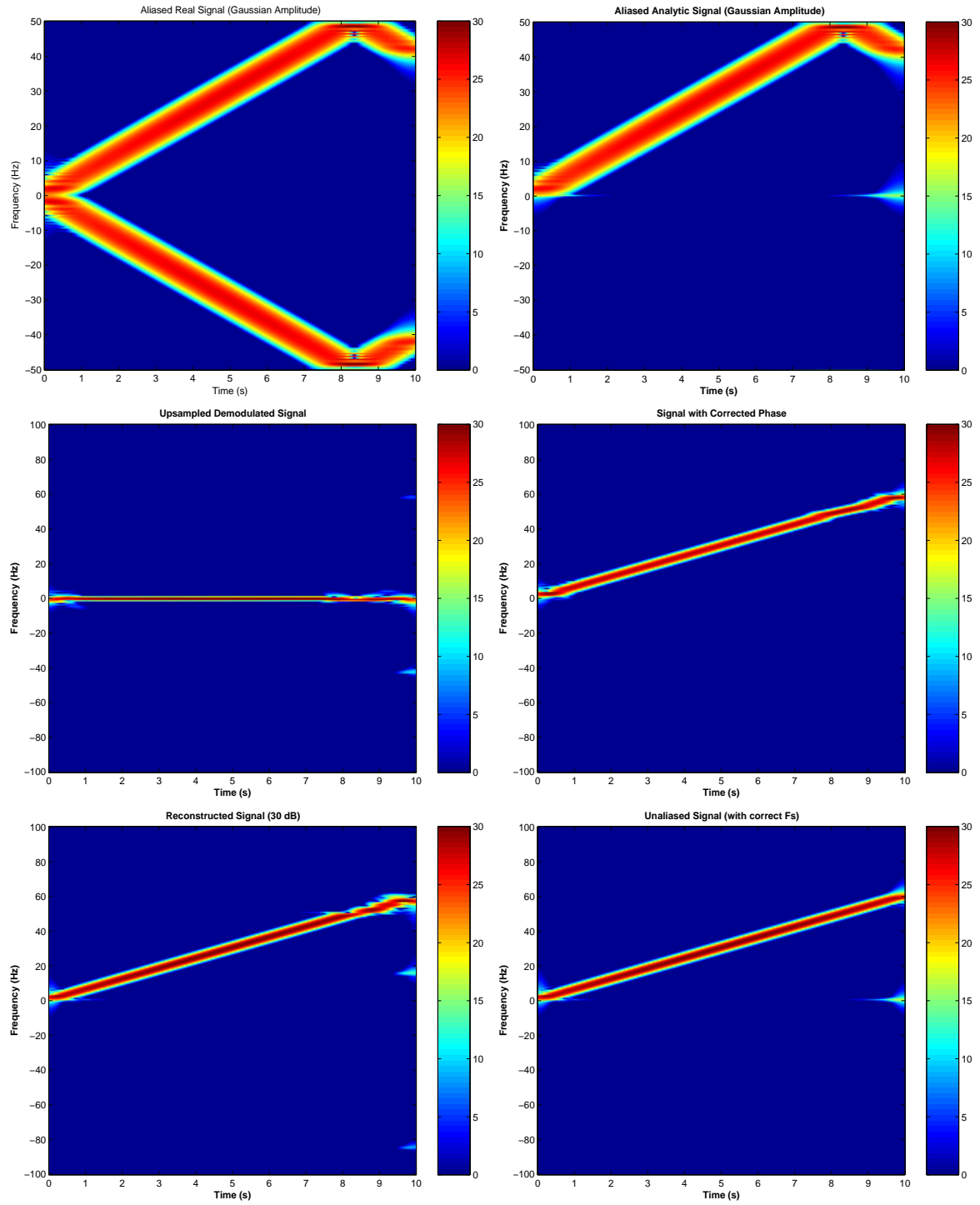


Figure 4.7: Case 1: Gaussian Amplitude, Log-magnitude spectrogram of (a) the aliased signal, (b) the analytic signal, (c) demodulated signal, (d) phase signal with corrected phase, (e) reconstructed signal and (f) unaliased signal (with correct sampling rate)

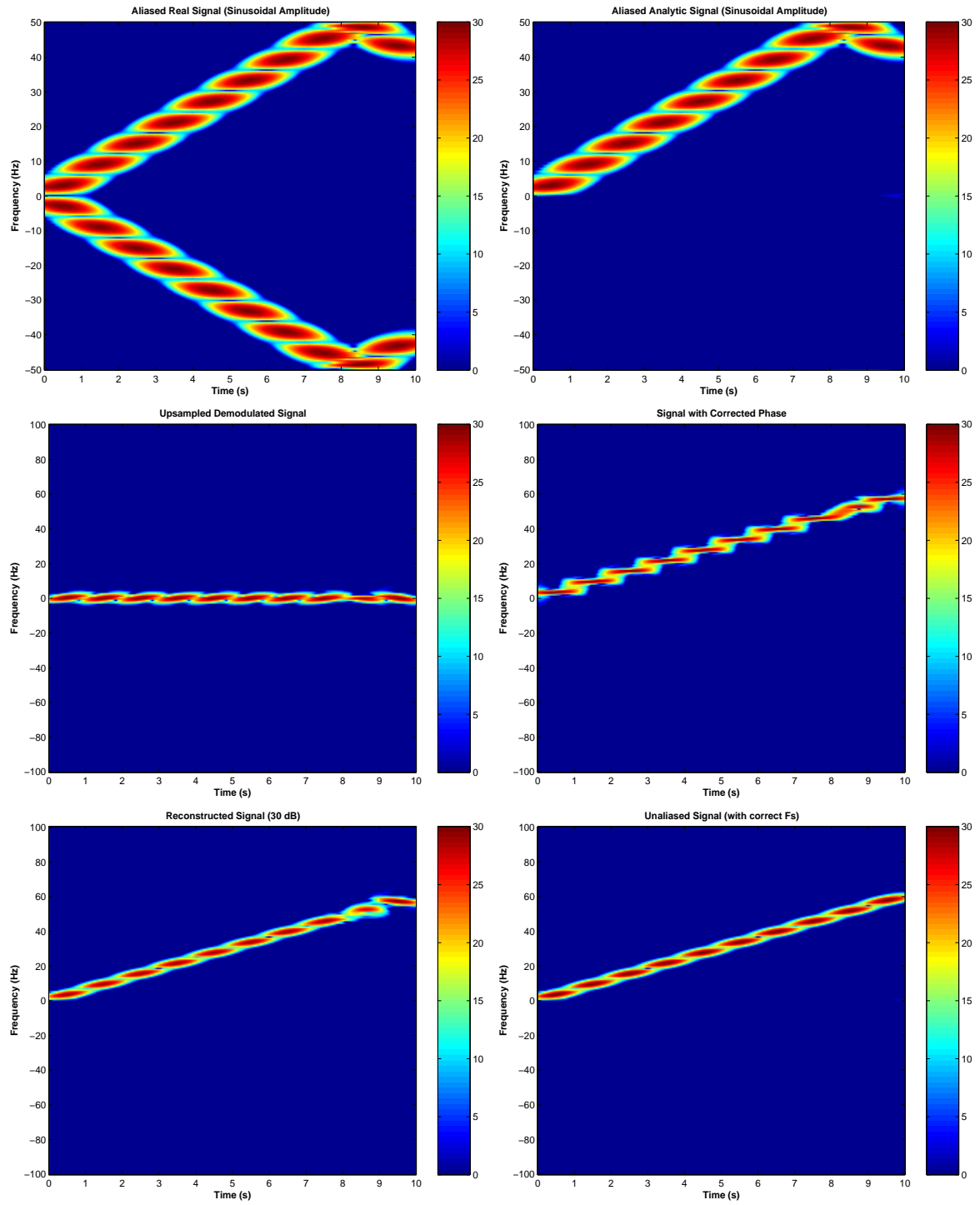


Figure 4.8: Case 2: Sinusoidal Amplitude, Log-magnitude spectrogram of (a) the aliased signal, (b) the analytic signal, (c) demodulated signal, (d) phase signal with corrected phase, (e) reconstructed signal and (f) unaliased signal (with correct sampling rate)

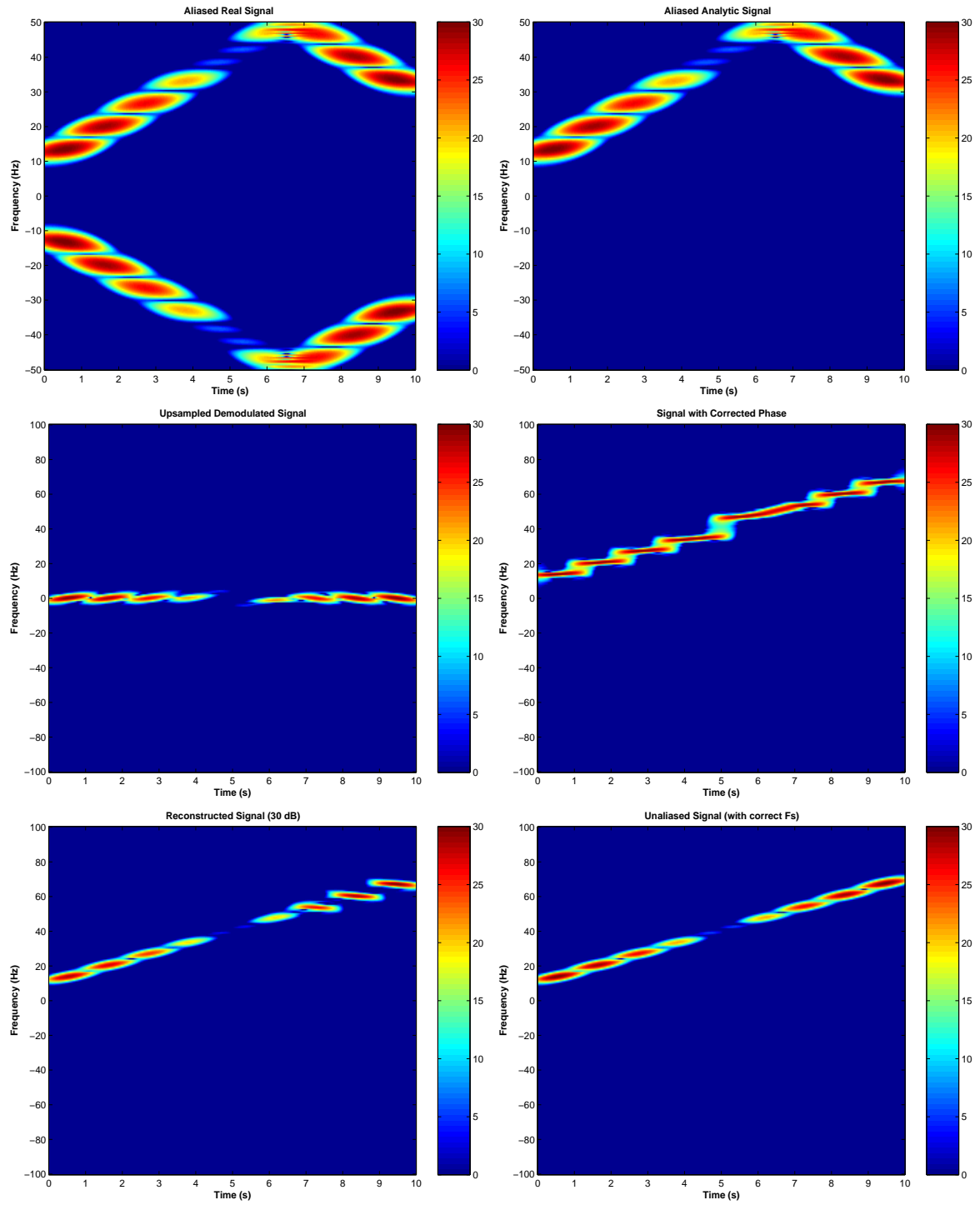


Figure 4.9: Case 3: Amplitude as a Combination of Sinusoids : Log-magnitude spectrogram of (a) the Aliased signal, (b) the analytic signal, (c) demodulated signal, (d) phase signal with corrected phase, (e) reconstructed signal and (f) unaliased signal (with correct sampling rate)

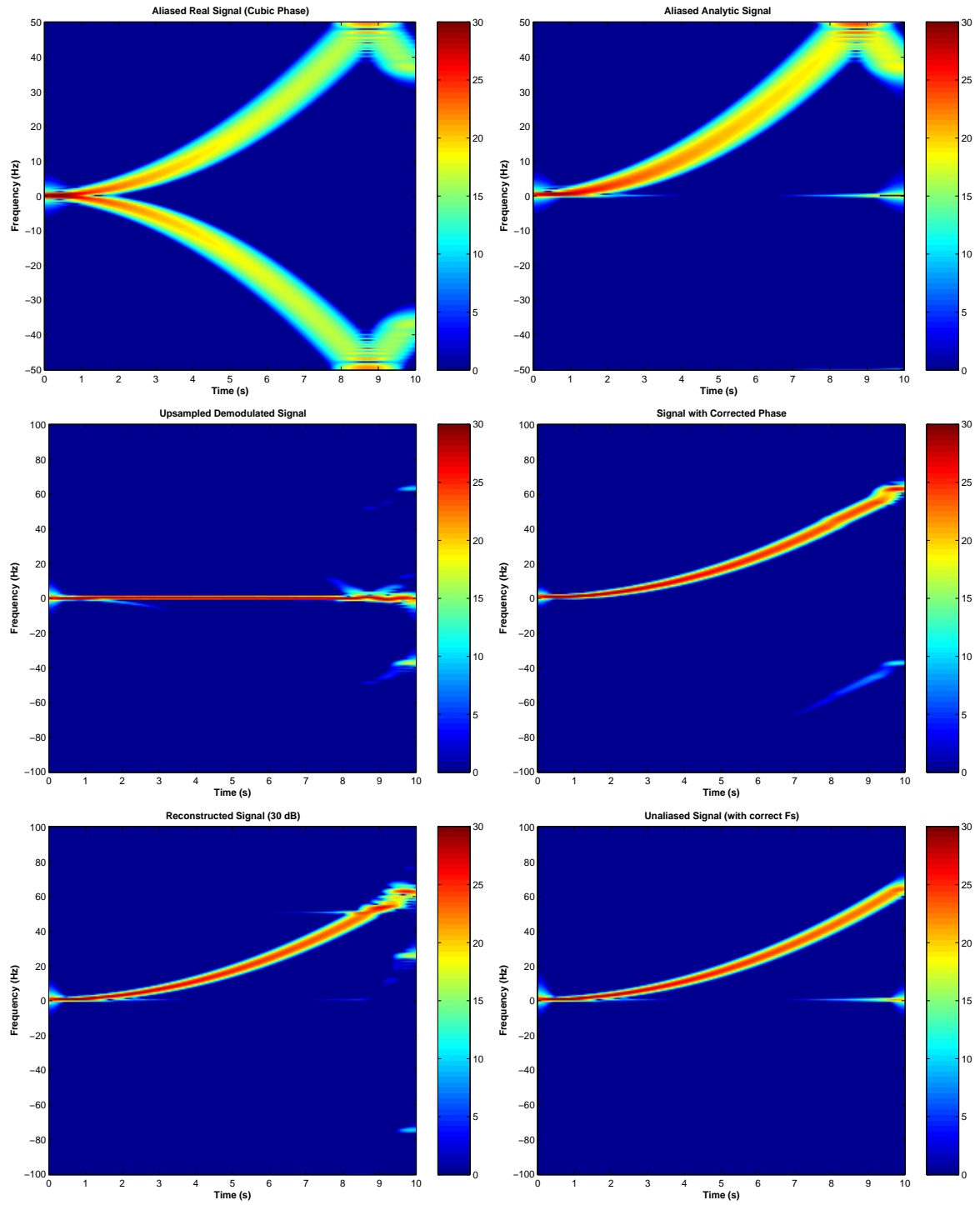


Figure 4.10: Case 4: Cubic Phase, Log-magnitude spectrogram of (a) the Aliased signal, (b) the analytic signal, (c) demodulated signal, (d) phase signal with corrected phase, (e) reconstructed signal and (f) unaliased signal (with correct sampling rate)

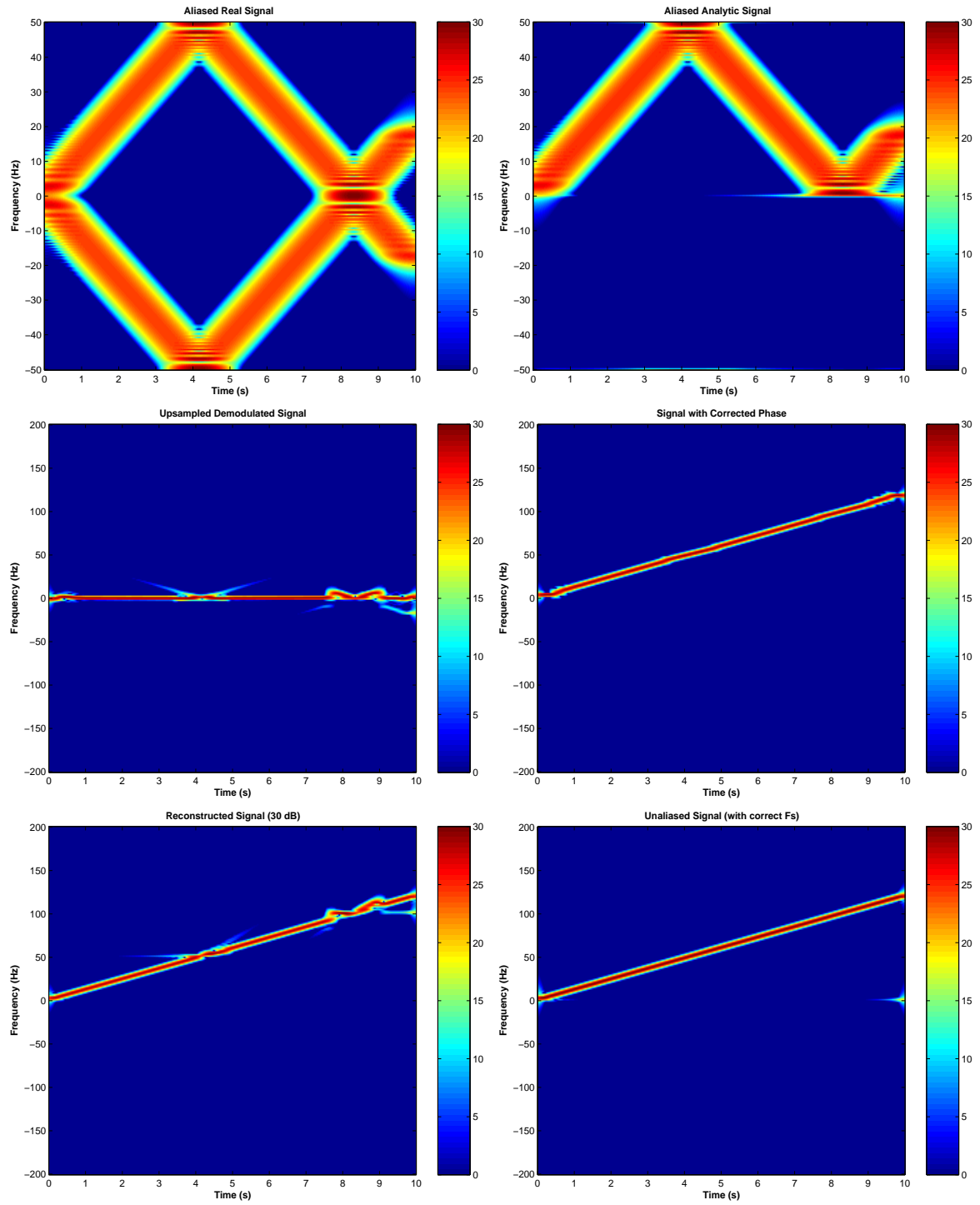


Figure 4.11: Case 6: Aliasing with Multiple Turns, Log-magnitude spectrogram of (a) the aliased signal, (b) the analytic signal, (c) demodulated signal, (d) phase signal with corrected phase, (e) reconstructed signal and (f) unaliased signal (with correct sampling rate)

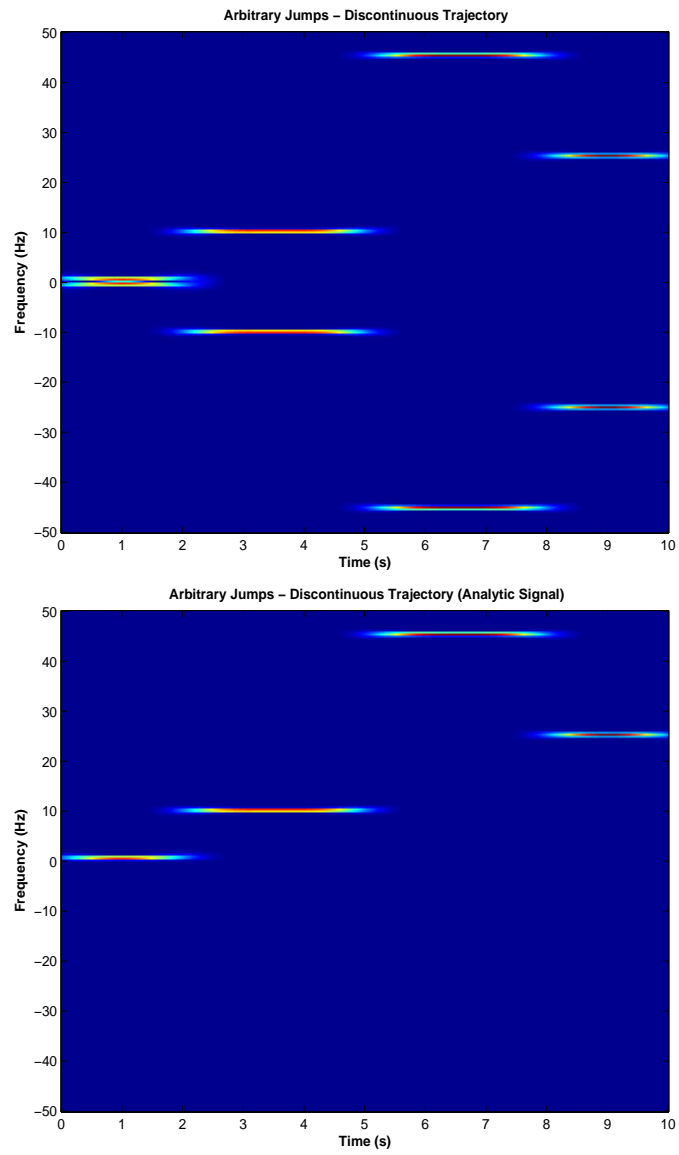


Figure 4.12: Log-magnitude spectrogram of (a) Signal with discontinuous trajectory and (b) its analytic signal

4.4 ANALYSIS OF “TURNS” IN IF

In this thesis we presented a method which attempts to identify aliasing in real signals by taking into account the “turns” in IF at the boundaries. Here a quantitative analysis for the IF turns is given which explains how we decide when the aliasing occurs.

Figure (4.13) shows an aliased analytic signal. The ideal IF for this signal and its first derivative are shown in figure (4.14).

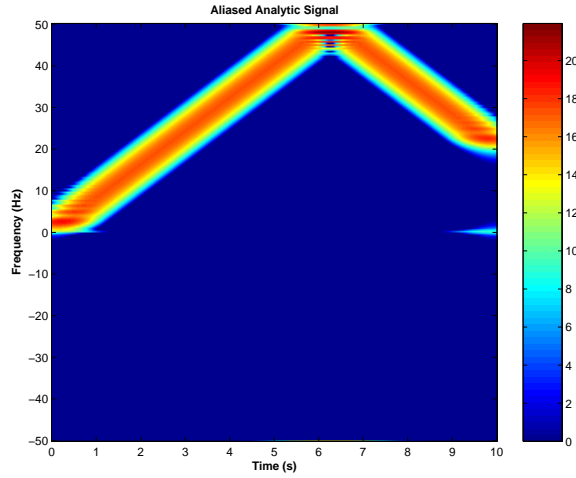


Figure 4.13: *Aliased analytic signal*

We can see clearly that the point where the aliasing occurs in the analytic signal coincides with the point where the differential of the IF changes sign.

We now consider an unaliased analytic signal shown in figure (4.15). The ideal IF for this signal and its derivative are also shown in the figure. In this case, the derivative is continuous and remains positive, reiterating that there were no sudden turns in IF and thus no aliasing.

Now consider the non-ideal cases, i.e. where we obtain the IF estimates from the spectrogram. The first derivative of the original IF estimates for the aliased analytic signal

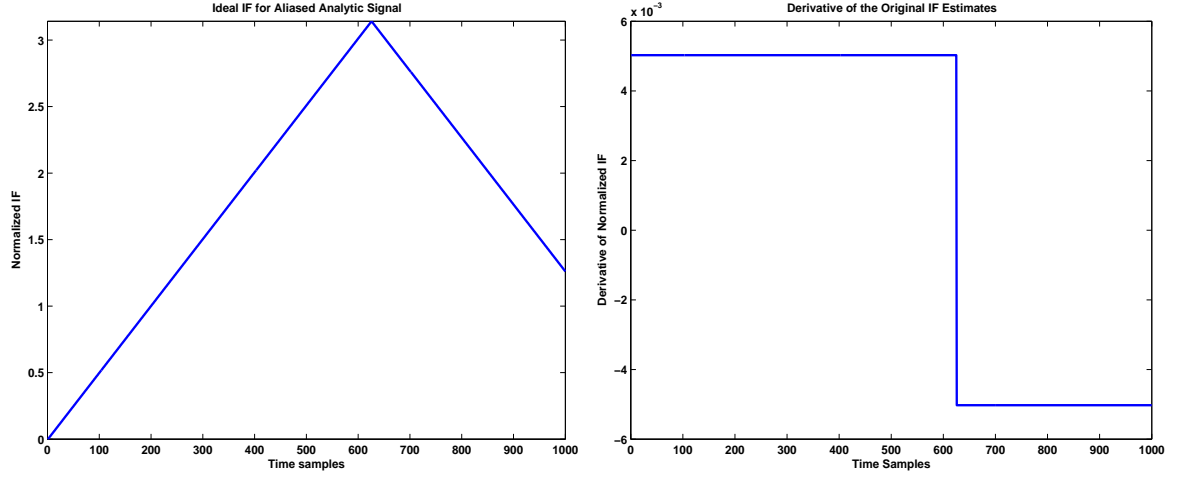


Figure 4.14: (a) *Ideal IF for the aliased signal* and (b) *its derivative*

(figure (4.13)) is shown in figure (4.16 (a)). Again, the figures agree with those for the ideal cases - aliasing occurs when the first derivative of IF changes signs.

In our method, we calculate the slope at each point of time. Under ideal conditions, the value of the slope at each point of time is different from the value at the previous time sample. But the IF estimates we obtain from the analytic-spectrogram method are not accurate and most of the times the IF follows a step pattern, i.e. it maintains a particular value for 3-4 time samples. Thus we obtain the derivative as shown in figure (4.16(a)). To overcome this and to see clearly the point of aliasing, we modify the derivative of the IF by partitioning the zero values (between every 2 non-zero values) into two parts and equating the first part to the earlier non-zero value and the second half to the next non-zero value. The smoothed version of the original IF is shown in figure (4.16).

Similarly, the first derivative of the corrected IF estimates and its smoothed version are shown in figure (4.17).

To further illustrate this point, we show the IF estimates and its smoothed derivative of

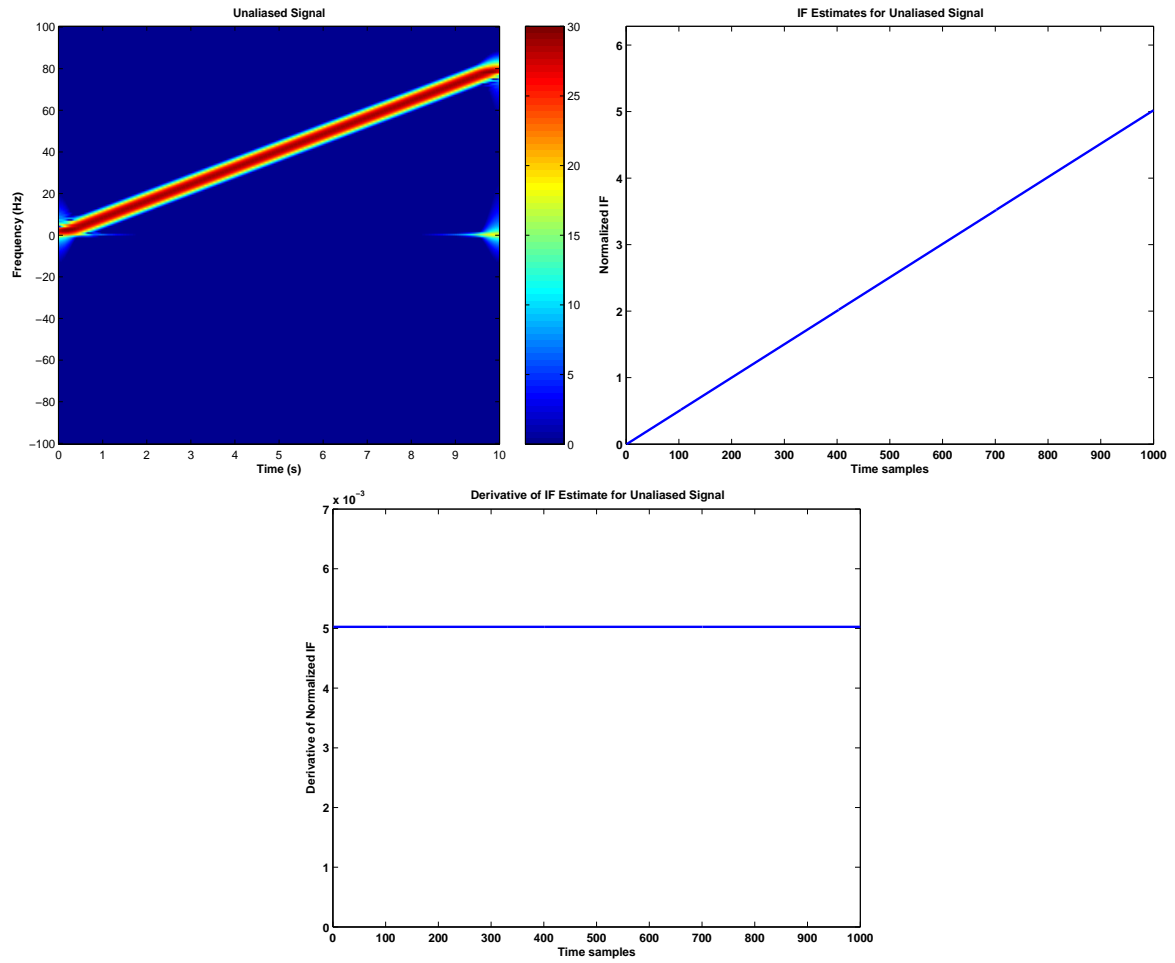


Figure 4.15: (a) *Unaliased analytic signal*, (b) *its ideal IF* and (c) *first derivative of IF*

an aliased sinusoidal amplitude chirp in figure (4.18).

Another alternative was to obtain all the points where the IF reached the maximum and the minimum values. If there were points after these extremals (in time) where the IF values were lower (higher) than the maximum (minimum) values, we consider aliasing to have taken place. The number of times such cases are obtained gives the number of potential turns in the IF. Both methods give perfect results for all types of signals which show such aliasing.

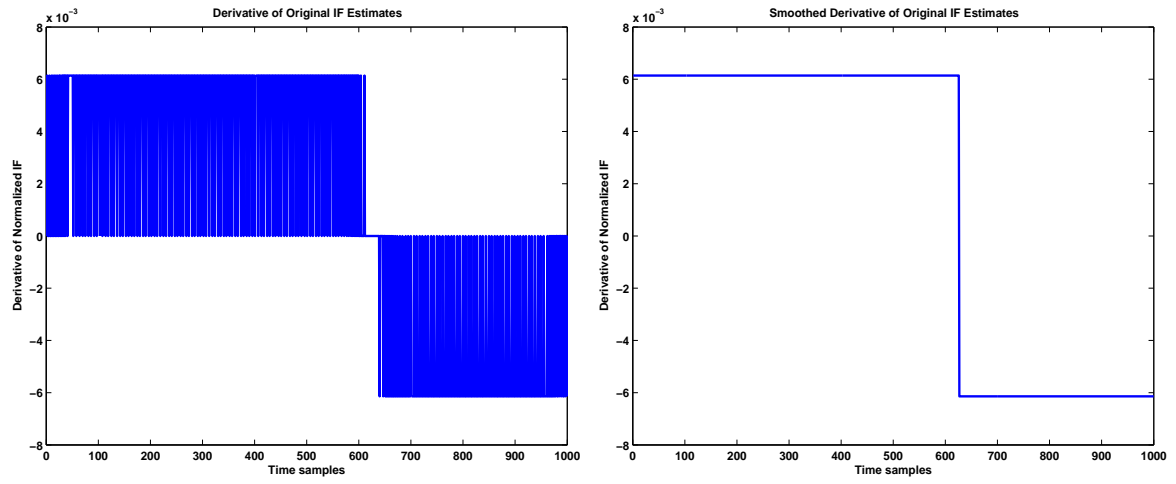


Figure 4.16: (a) First derivative of the original IF estimates and (b) its “smoothed” version

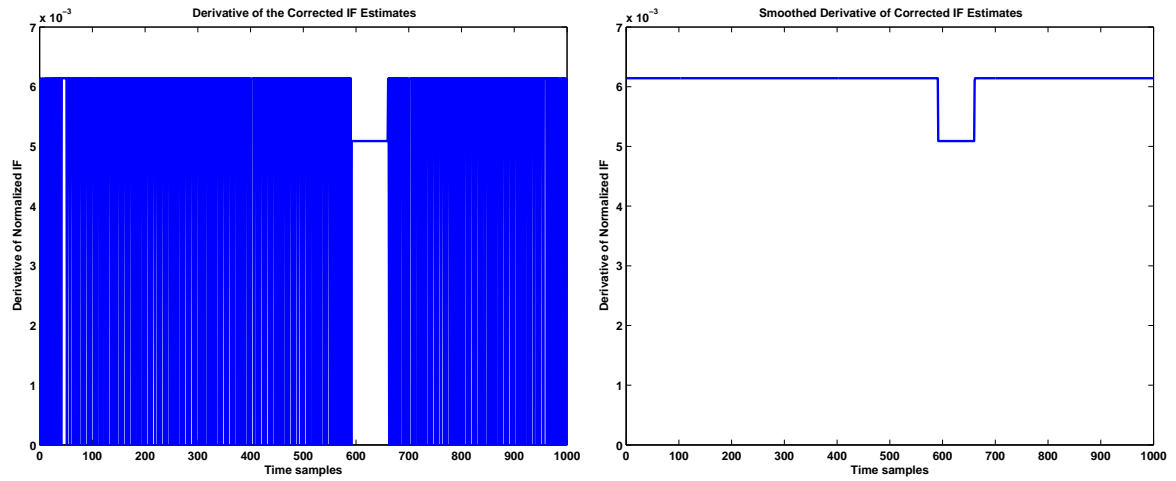


Figure 4.17: (a) First derivative of the corrected IF estimates and (b) its “smoothed” version

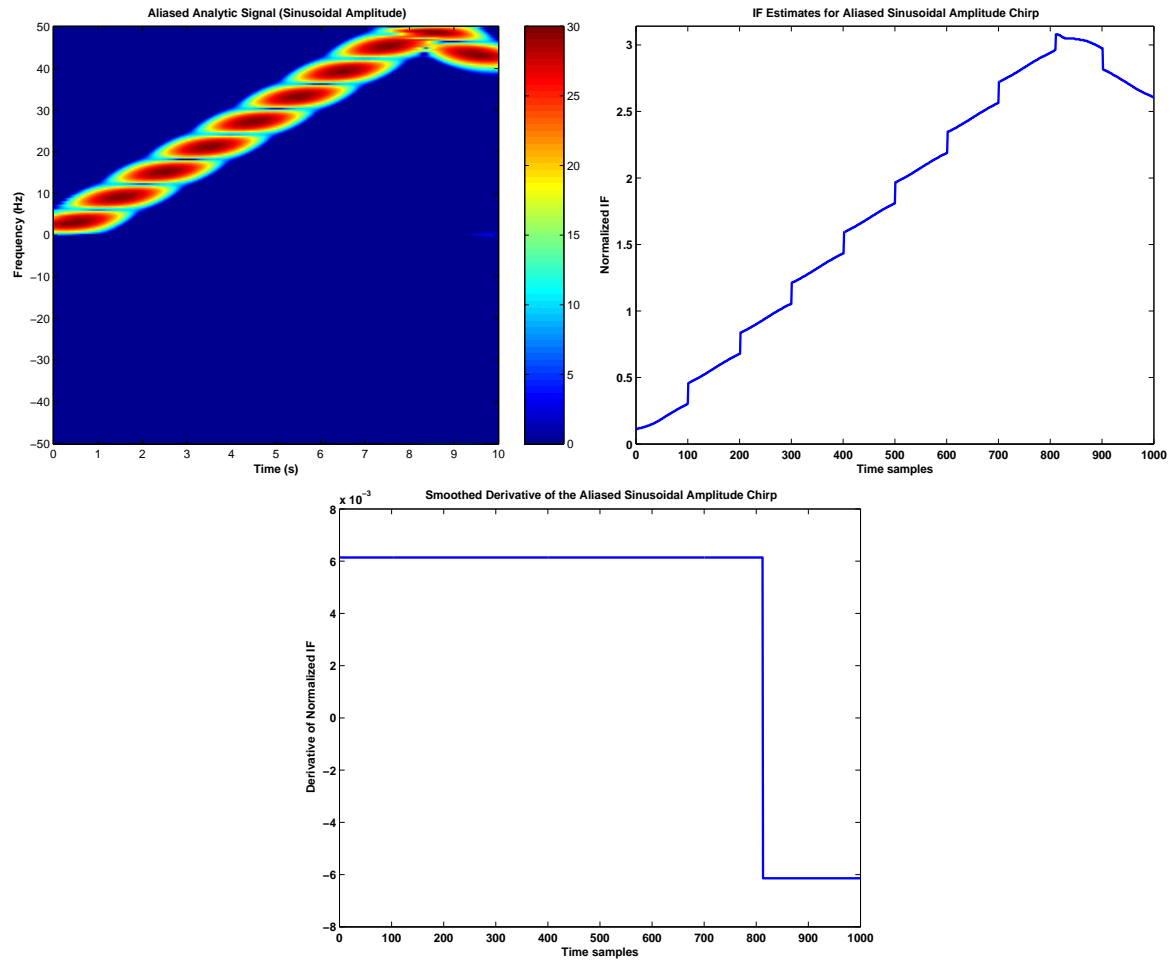


Figure 4.18: (a) Sinusoidal amplitude aliased analytic signal, (b) its IF estimates and (c) smoothed first derivative of the IF estimate

4.5 APPLICATION : MULTI-COMPONENT SIGNALS

This method can be extended to multi-component signals. The steps to be followed are explained here using an example of an aliased two-component signal given by:

$$x(t) = 15\cos(2\pi t^2) + 25\cos(2\pi(10t + 2.5t^2))$$

The aliased real and analytic signals are shown in figure (4.19). Here again for our calculations we use ideal IF estimates.

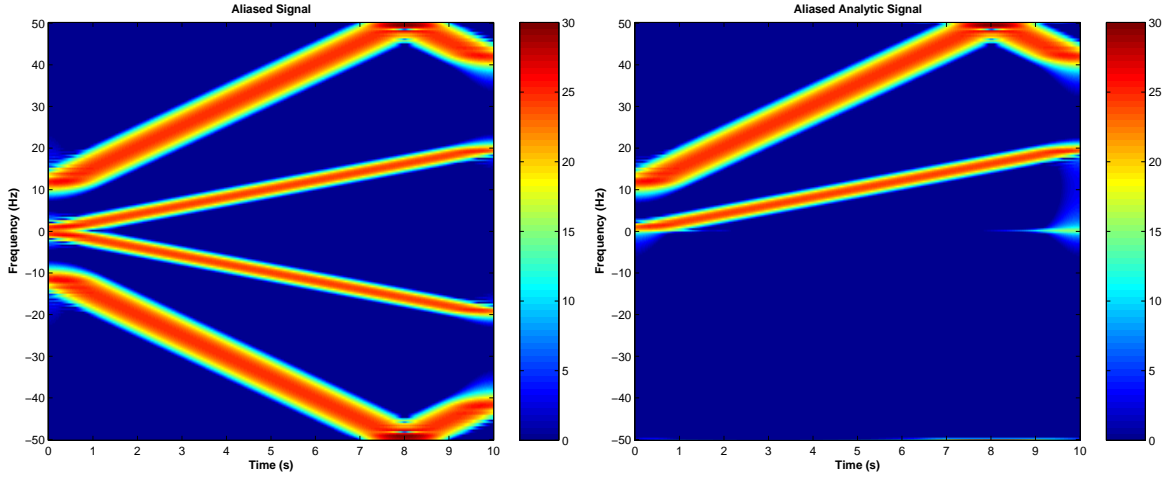


Figure 4.19: *Combination of two chirps: Log-magnitude spectrogram of (a)aliased analytic signal and (b)the analytic signal*

1. Estimate IF and phase for the first component, demodulate this component and low-pass filter the demodulated signal. Estimate the corrected IF and phase and upsample the demodulated signal and the phase and then use them to remodulate to obtain the first reconstructed signal component. The results for this step are shown in the figure (4.20)
2. Repeat the previous step for the second component. The results for the second component are shown in the figure (4.21)

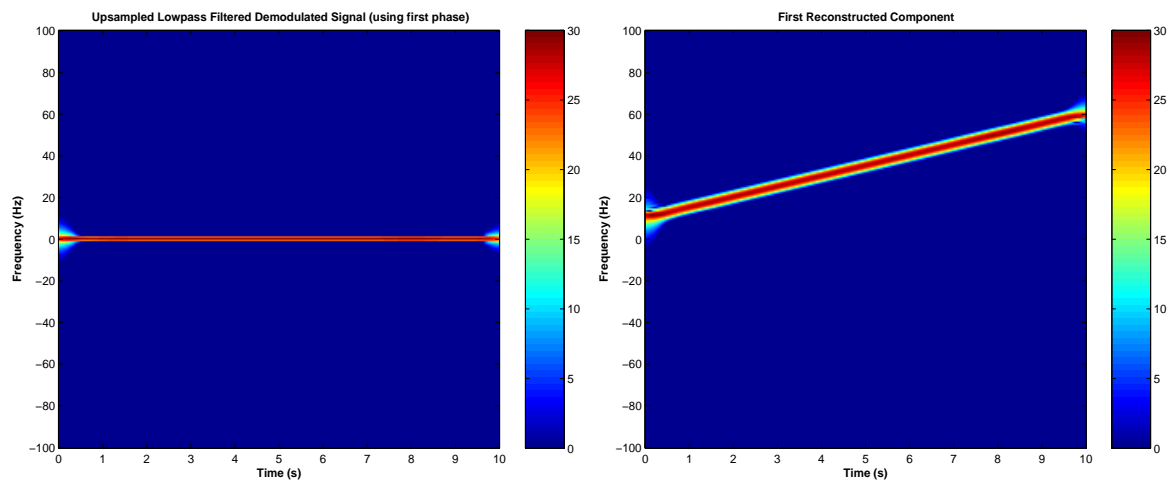


Figure 4.20: *Combination of two chirps: Log-magnitude spectrogram of (a) the upsampled low-pass filtered demodulated signal using first phase, and (b) the first reconstructed chirp component*

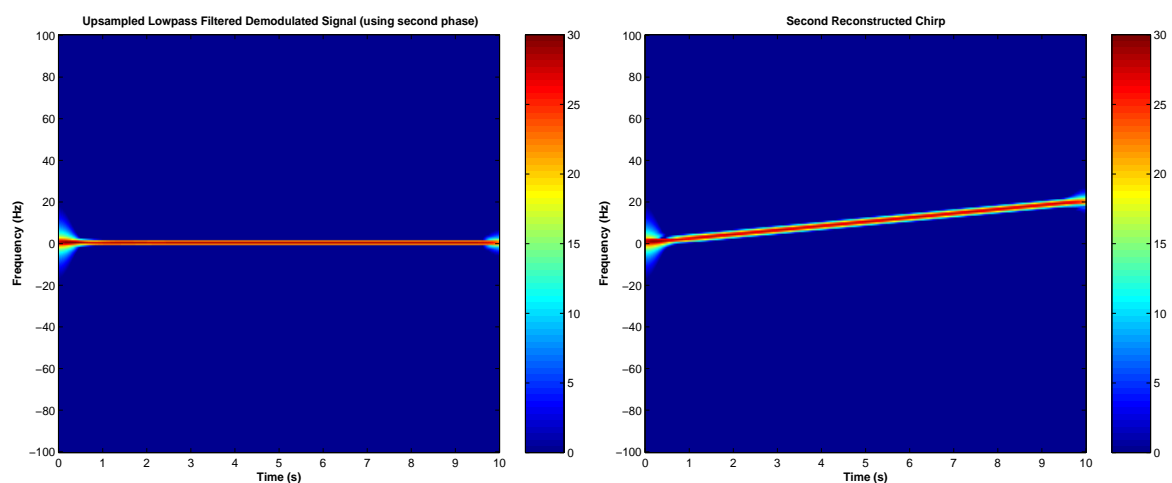


Figure 4.21: *Combination of two chirps: Log-magnitude spectrogram of (a) the upsampled low-pass filtered demodulated signal using second phase, and (b) the second reconstructed chirp component*

3. Add the two reconstructed components to obtain the final reconstructed signal as shown in figure (4.22).

The results were then compared to the original unaliased signal and the errors are shown in figure (4.23). From these figures, it is clear that it is possible to extend our method

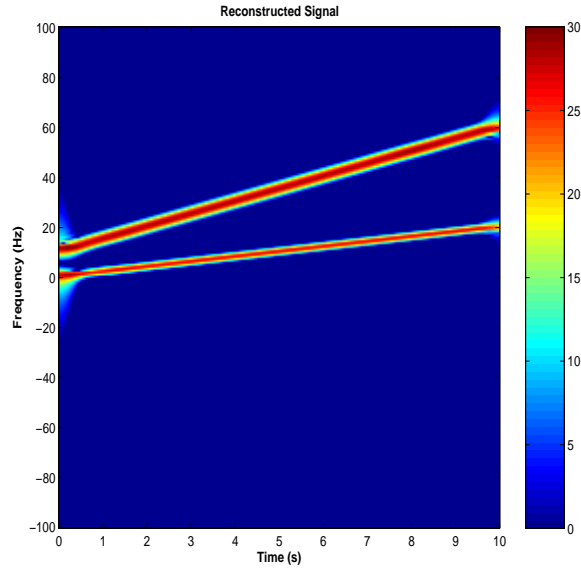


Figure 4.22: *Combination of two chirps: Log-magnitude spectrogram of the reconstructed signal*

to multi-component signals by estimating the IF of each component, and demodulating and filtering each component separately, then correcting the components and reconstructing the signal from the corrected components. These examples show that with more elaborate techniques for separating the components, and accurate IF estimates, accurate results can be obtained for restoring aliased multi-component signals.

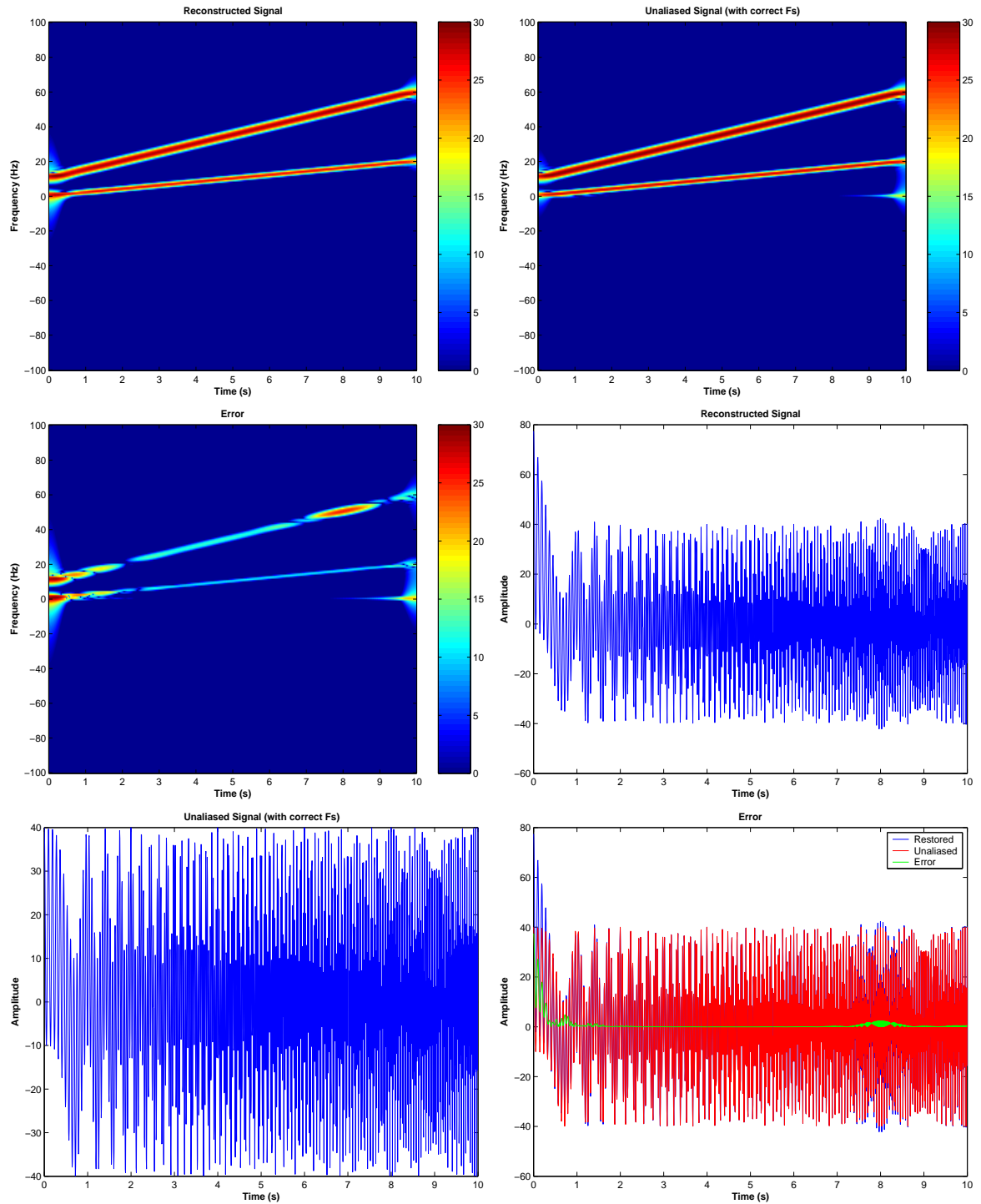


Figure 4.23: *Combination of two chirps: (a) Log-magnitude spectrogram of the restored signal (b) log-magnitude spectrogram of the “true” unaliased signal (with correct sampling rate) (c) error between (a) and (b). Time-series of the (d) reconstructed signal, (e) “true” unaliased signal (with correct sampling rate) and (f) the error between (d) and (e)*

4.6 IF ESTIMATE AND OTHER SOURCES OF ERROR

As seen from the examples illustrating the ideal IF cases, it is clear that the results were significantly improved as the IF estimate became better. In our method the window of the spectrogram had a significant affect on the IF estimates obtained. For future work we could focus on other techniques for IF estimations to obtain the one which gives almost ideal results for IF.

But even in ideal conditions, we did not obtain perfect results. This could be due to the analytic signal calculations. This is true because when we developed our method for quadrature signals, which does not require analytic signal calculations, we obtained perfect results using the same code (figures (4.24,4.25)).

In this thesis we introduced a method which challenged the long standing notion that once sampled at a rate lower than the sampling rate, the signal cannot be retrieved. We presented the idea that by estimating the IF for certain signals, we can possibly identify and compensate for aliasing. We showed this using both ideal and estimated IF. We also demonstrated that the idea could be extended to multi-component signals.

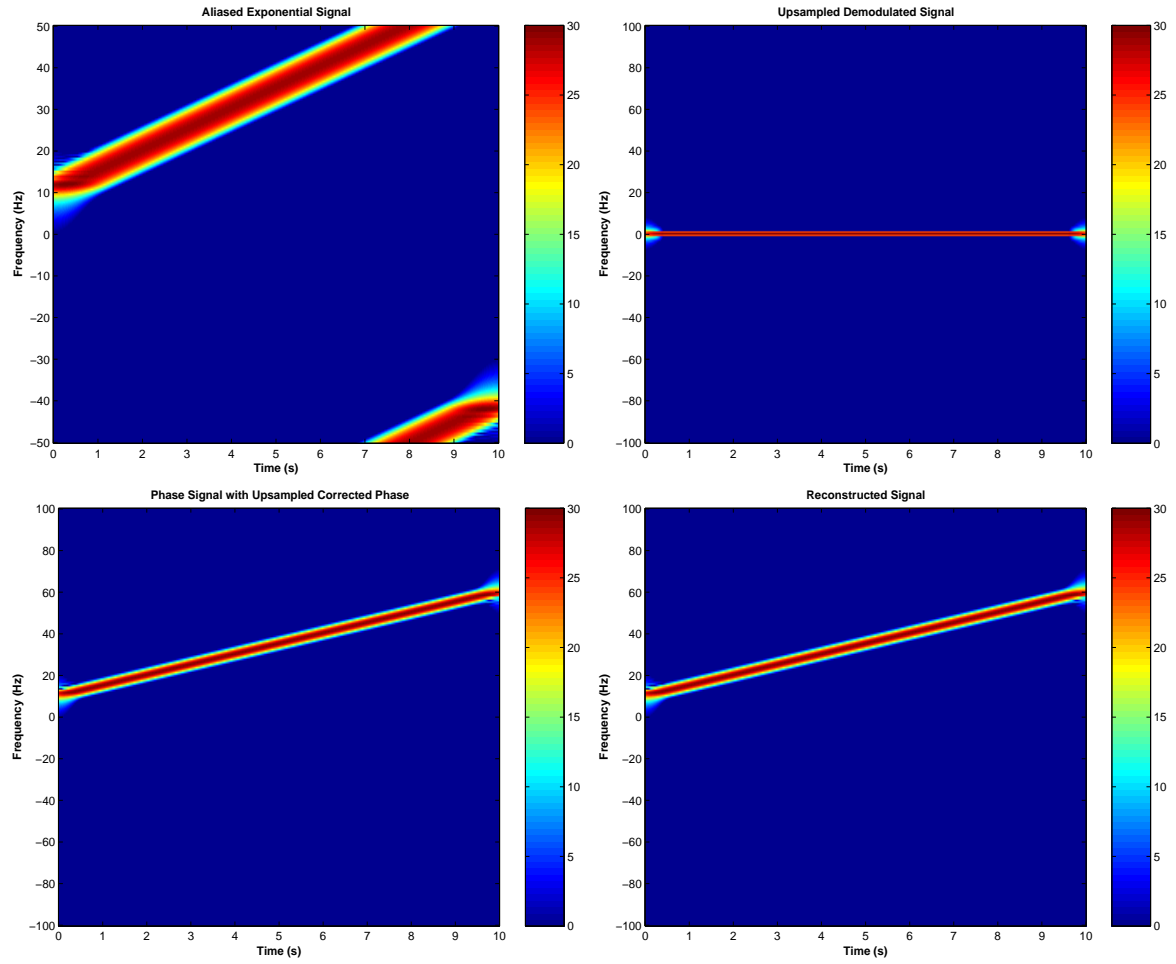


Figure 4.24: *Quadrature Signal : Log-magnitude spectrogram of (a) the aliased signal, (b) upsampled demodulated signal, (c) phase signal with corrected phase and (d) reconstructed signal*

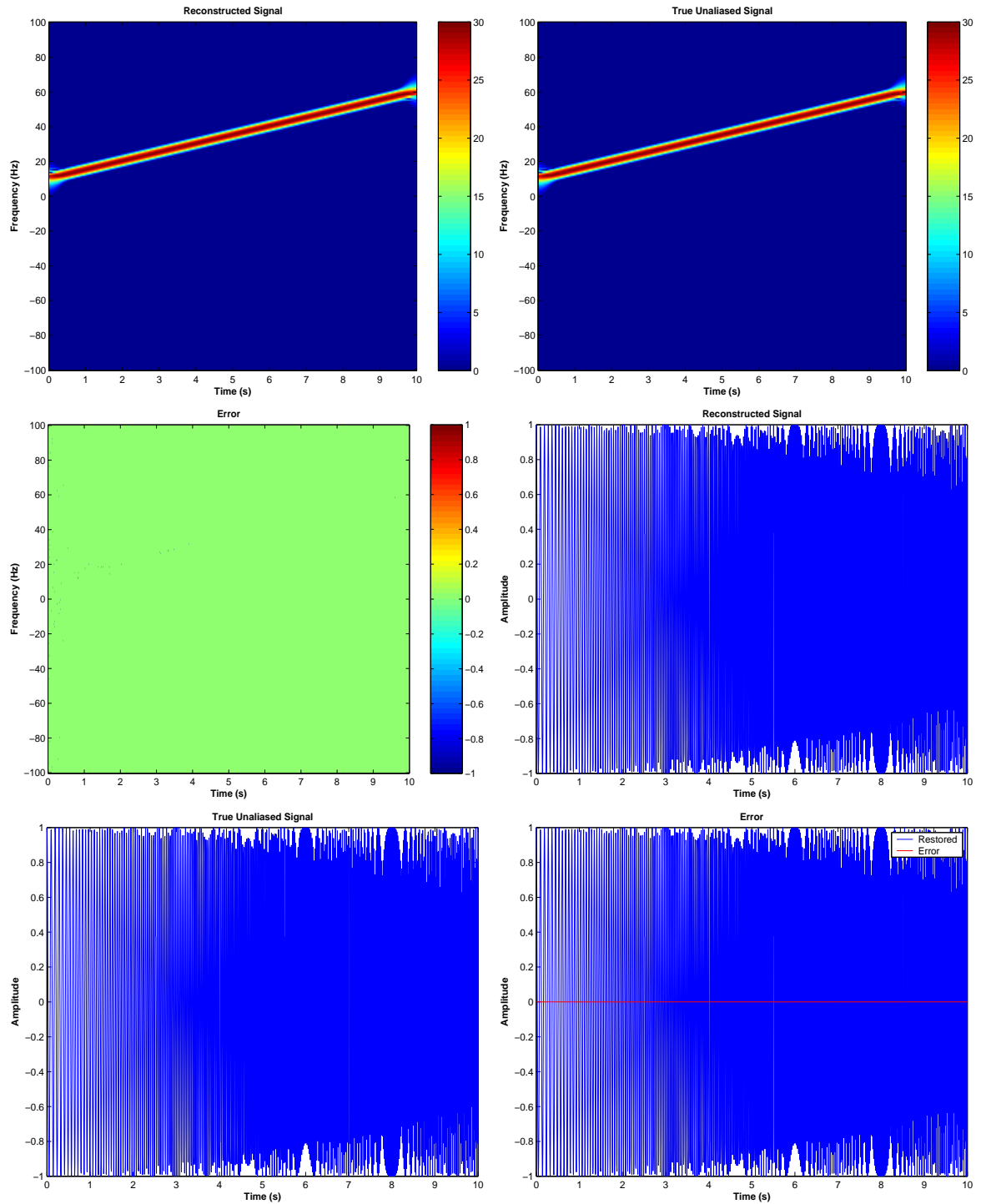


Figure 4.25: Quadrature Signal : (a) Log-magnitude spectrogram of the restored signal (b) log-magnitude spectrogram of the “true” unaliased signal (with correct sampling rate) (c) error between (a) and (b). Time-series of the (d) reconstructed signal, (e) “true” unaliased signal (with correct sampling rate) and (f) the error between (d) and (e)

APPENDIX

SOURCE CODE

```
function [y_r,n,str] = aliasing(x)
%%%%%%%%%%%%%%%%%%%%%%%%%%%%%%%%%%%%%%%%%%%%%%%%%%%%%%%%%%%%%%%%%%%%%%%%
% Function for identifying and compensating for aliasing
%   Input parameters:
%       x : input signal
%   Output parameters:
%       str : string specifying "aliasing" or "no aliasing"
%       n : number of sudden turns
%       y_r: reconstructed signal (same as input signal
%                                   in case of no aliasing)
% Aasma Walia, M. S. Thesis under the guidance of Prof. P. J. Loughlin

y=hilbert(x); % analytic signal
sg=sgram2(y,256,255,1);
[T,F]=size(sg); % time & frequency vectors for plots
T=0:T-1; F=0:F-1;
m=(2*pi)/(F(length(F))-F(1)); %convert freq. vector from bins to samples
b=-pi-m*F(1); F=m*F+b; [A, k] = max(sg') ;
for i=2:1:length(k) % frequency estimates
    if abs(F(k(i))-F(k(i-1)))>2
        sg(i,k(i))=0;
        [A,k]=max(sg');
    end;
end;
[A,k]=max(sg'); L=[];
for I = 1:1:length(k)
    L=[L F(k(I))];
end;
L1=L; LL=L; n=0;
[c,l]=max(L1);
p=find(L1<max(L1));
m=find(p>1);
```

```

while(m)
    n=n+1;L=L1;
    [A,i]=max(L);
    i=find(L==A);
    L1=L(1:min(i)-1);
    Lm=LL;LL=L1;k=min(i);
    Value=(n*pi-L(min(i)-1))/((max(i)+min(i))/2-((min(i))))
    while k<=(min(i)+max(i))/2
        LL=[LL LL(k-1)+Value];
        k=k+1;
    end;
    while k<=max(i)+1 & k<=length(L)          % modify IF estimates
        LL=[LL LL(k-1)-Value];                % for windowing errors
        k=k+1;
    end;
    LL=[LL L(max(i)+2:length(L))];
    if LL(max(i)+2)>LL(max(i)+1)
        LL=L;
    end;
    k=min(i);
    while k<=max(i)+1 & k<=length(L)          % correct IF estimates
        L1=[L1 L1(k-1)+Value];
        k=k+1;
    end;
    L1=[L1 (n*pi-L(max(i)+2:length(L))+n*pi)];
    [c,l]=max(L1);p=find(L1<max(L1)); m=find(p>1);
    if n==1
        Lm=LL;
    end;
end;
IF_o=Lm;                                     % modified IF estimates
IF_c=L1;                                     % corrected IF estimates
if(n==0)
    str='no aliasing'
    y_r=x;
else
    str='aliasing occurs'
    Phi_Hat=cumsum(IF_o);
    y1=exp(-j*Phi_Hat);
    y_d=y.*y1;
    Phi_Hat_Hat=cumsum(IF_c);
    Phi_Corrected=interpolate(Phi_Hat_Hat,n);
    y_d_u=interpolate(y_d,n);
    y_r=y_d_u.*exp(j*Phi_Corrected);
end;

```

```

function [result] = interpolate(input,n)
%%%%%%%%%%%%%%%%%%%%%%%%%%%%%%%%%%%%%%%%%%%%%%%%%%%%%%%%%%%%%%%%%%%%%%%%%%%%%%
% Function for upsampling the input by 2*n
%   Input parameters:
%       input : input signal
%       n : for 2*n upsampling rate
%   Output parameters:
%       result : upsampled signal (2*n-1)
%               times longer than input
% Aasma Walia, M. S. Thesis under the guidance of Prof. P. J. Loughlin

input1=input; for k=1:n
    result=[];
    for i=1:length(input)-1
        result=[result input1(i) (input1(i)+input1(i+1))/2];
    end;
    result=[result input1(length(input1))];
    input1=result;
end;

```

BIBLIOGRAPHY

- [1] E. C. Bekir. Unaliased discrete-time ambiguity function. *Journal of Acoustical Society of America*, 93:363–371, January 1993.
- [2] G. F. Boudreaux-Bartels and T. W. Parks. Reducing aliasing in the wigner distribution using implicit spline interpolation. In *IEEE International Conference on Acoustics, Speech and Signal Processing*, volume 8, pages 1438–1441, April 1983.
- [3] John R. Carson and Thornton C. Fry. Variable frequency electric circuit theory with application to the theory of frequency-modulation. *Bell System Technical Journal*, 16:513–540, 1937.
- [4] David S. K. Chan. A non-aliased discrete-time wigner distribution for time-frequency signal analysis. In *IEEE International Conference on Acoustics, Speech and Signal Processing*, volume 7, pages 1333–1336, May 1982.
- [5] T. A. C. M. Classen and W. F. G. Meckenbrauker. The wigner distribution-tool for time-frequency signal analysis-part ii. *Philips Research Journal*, 35, 1980.
- [6] T. A. C. M. Classen and W. F. G. Meckenbrauker. The wigner distribution-tool for time-frequency signal analysis-part iii. *Philips Research Journal*, 35, 1980.
- [7] Leon Cohen. *Time-Frequency Signal Analysis*, chapter Introduction: A Primer on Time-Frequency Analysis.
- [8] Leon Cohen. Time-frequency distributions-a review. *Proceedings of the IEEE*, 77, July 1989.
- [9] Antonio H. Costa and G. F. Boudreaux-Bartels. A comparative study of alias-free time-frequency representations. In *Proceedings of IEEE-SP International Symposium on Time-Frequency and Time-Scale Analysis*, pages 76–79, October 1994.
- [10] Antonio H. Costa and G. F. Boudreaux-Bartels. An overview of aliasing errors in discrete-time formulations of time-frequency representations. *IEEE Transactions on Signal Processing*, pages 1463–1474, May 1999.
- [11] B. Van der Pol. The fundamental principles of frequency modulation. *Proceedings of IEE*, 93, 1946.

- [12] Gerard C. A. Fonte. Breaking the nyquist barrier : A new signal processing technique.
- [13] D. Gabor. Theory of communications. *IEE Journal of Communication Engineering*, 93, 1946.
- [14] J. Jeong and W. J. Williams. Alias-free generalized discrete-time time-frequency distributions. *IEEE Transactions on Signal Processing*, 40:2757–2765, November 1992.
- [15] Jechang Jeong and William J. Williams. A new formulation of generalized discrete-time time-frequency distributions. In *IEEE International Conference on Acoustics, Speech and Signal Processing*, volume 5, pages 3189–3192, April 1991.
- [16] P. J. Loughlin. Do bounded signals have bounded amplitudes? *Multidim. Syst. Signal Processing*, 9:419–424, 1998.
- [17] Patrick J. Loughlin and Berkant Tacer. On the amplitude- and frequency-modulation decomposition of signals. *Journal of Acoustical Society of America*, 100, September 1996.
- [18] Joel M. Morris and Dongsheng Wu. On alias-free formulations of cohen’s class of distributions. *IEEE Transactions on Signal Processing*, pages 1355–1364, June 1996.
- [19] A. H. Nuttall. Alias-free wigner distribution function and complex ambiguity function for discrete-time samples. *NUSC Technical Report 8533*, April 1989.
- [20] J. O’Hair and B. Suter. Kernel design techniques for alias-free time-frequency distributions. *IEEE International Conference on Acoustics, Speech and Signal Processing*, pages III.333–336, April 1994.
- [21] F. Peyrin and R. Prost. A unified definition for the discrete-time, discrete-frequency, and discrete-time/frequency wigner distributions. *IEEE Transactions on Acoustics, Speech, and Signal Processing*, 34:858–867, August 1986.
- [22] Bernard Pincinbono. On instantaneous amplitude and phase of signals. *IEEE Transactions on Signal Processing*, 45, March 1997.
- [23] LJubiša Stanković and Igor Djurović. A note on ”an overview of aliasing errors in discrete-time formulations of time-frequency representations”. *IEEE Transactions on Signal Processing*, pages 257–259, January 2001.
- [24] David Vakman. On the analytic signal, the teager-kaiser energy algorithm, and other methods for defining amplitude and frequency. *IEEE Transactions on Signal Processing*, 44(4), April 1996.
- [25] H. K. Dunn W. Koenig and L. Y. Lacy. The sound spectrograph. *Journal of Acoustical Society of America*, 18:S.19–49, 1946.